Design optimization of a gearbox driven tidal stream turbine

Khalil Touimi

DOCTORAT BRETAGNE SCIENCES LOIRE POUR L'INGENIEUR

Université de Bretagne Occidentale

THESE DE DOCTORAT DE

L'UNIVERSITE
DE BRETAGNE OCCIDENTALE

ECOLE DOCTORALE N° 602
Sciences pour l'Ingénieur
Spécialité : *Génie électrique*

Par

Khalil TOUIMI

Design Optimization of a Gearbox Driven Tidal Stream Turbine.

Thèse présentée et soutenue à Brest, le 23 Juin 2020
Unité de recherche : UMR CNRS 6027 IRDL – Institut de Recherche Dupuy de Lôme

Rapporteurs avant soutenance :

Abdesslem DJERDIR	Professeur, UTBM
Jean-Philippe LECOINTE	Professeur, Université d'Artois

Composition du Jury :

Président :	
Claude MARCHAND	Professeur, Université Paris-Saclay
Examinateurs :	
Mostapha TARFAOUI	Professeur, ENSTA Bretagne
Anne BLAVETTE	Chargée de Recherche CNRS, ENS Rennes
Jean-Frédéric CHARPENTIER	Maître de Conférences – HDR, Ecole Navale
Abdesslem DJERDIR	Professeur, UTBM
Jean-Philippe LECOINTE	Professeur, Université d'Artois
Dir. de thèse :	
Mohamed BENBOUZID	Professeur, Université de Bretagne Occidentale

Invité(s)

Nicolas RUIZ	Ingénieur, Guinard Energies

To my father, my mother, my wife, and my children

Abstract

Abstract: Tidal stream energy is acquiring more and more attention as a future potential renewable energy source. However, tidal stream turbines are still in development stages and their technology is not as mature as wind turbine technology. In addition to the infancy of the technology, tidal stream turbines have to withstand the harsh submarine environment where they are immersed. These constraints increase the criticality of tidal stream turbine subsystems and make them less reliable. Therefore, improving the reliability presents one of the challenges to make such energy competitive in terms of cost compared to other types, notably wind and solar energy. Indeed, the tidal stream turbine reliability and the produced energy cost are mainly affected by the drivetrain and generator configuration choices. In this thesis, the suitable drivetrain and generator option choice is investigated for tidal stream turbine specifications. Three main generators and drivetrain configurations are considered which are, the direct-drive tidal stream turbine (gearless), the mechanically geared tidal stream turbine (two-stage and single-stage gearbox driven), and the magnetically geared one. The design process considers the electromagnetic modeling of the generator, the converter model, the turbine model, and the tidal current velocity data (near Ouessant island). The investigation results could be useful for tidal stream turbine designers and could give them a sight on the feasibility of each tidal stream turbine type.

Acknowledgements

My deepest appreciation goes to my supervisor, Professor Mohamed Benbouzid, for the continuos support of my PhD study and research, for his patience, motivation, wisdom, and immense knowledge.

I would like to offer my special thanks to the Military Polytechnic school (Ecole Militaire Polytechnique) in Algiers for providing me a postgraduate scholarship.

I would like also to thank my friends Zakaria Oubrahim, Tony El Tawil, Dhaffar Ibrahim, and Youness Trachi for their support at the beginning of my thesis.

I would like to particularly thanks Mohamed Fahed Zia, Nadir Boukoberine, and Abhinandana Boodi for the amazing moment we had together during my PhD.

Finally I owe a very important debt to my dear parents who supported me during all my scientific studies. I also owe my deepest gratitude to my dear wife for her love, support, and help. I also thank all who supported me during my stay in France.

List of Publications

Main results of this PhD thesis have lead to the following publications:

International journals:

1. K. Touimi, M. Benbouzid, and P. Tavner. Tidal stream turbines: With or without a gearbox?. Ocean Engineering, 2018, vol. 170, p. 74-88.
2. K. Touimi, M. Benbouzid, and Z. Chen. Optimal Design of a Multibrid Permanent Magnet Generator for a Tidal Stream Turbine. Energies, 2020, vol. 13, no 2, p. 487.

International conferences:

1. K. Touimi, M. Benbouzid, and P. Tavner. A Review-based Comparison of Drivetrain Options for Tidal Turbines. In : 2018 IEEE International Power Electronics and Application Conference and Exposition (PEAC). IEEE, 2018. p. 1-6.

Contents

List of Figures

List of Tables

List of Abbreviations and Parameters

TST	Tidal stream turbine
DD	Direct-drive
PMG	Permanent magnet generator
AEP	Annual energy production
PWM	Pulse width modulation
P_T	Input shaft power
A_t	Turbine blade swept area
ρ	Sea water density
C_p	Power coefficient
$D_{turbine}$	Turbine diameter (blades)
λ	Tip speed ratio
λ_{opt}	Optimum tip speed ratio
β	Pitch angle
v_a	Current velocity amplitude
$\theta_{current}$	Current angular direction
θ_{opt}	Optimal current angular direction
v_i	Cut-in tidal current speed
v_c	Cut-out tidal current speed
v_n	Rated tidal current speed
P_{Tr}	Rated input shaft power
P_{max}	Maximum input shaft power
OCC	Occurrence frequency
FW	Gear face width

d_s	Sun gear diameter
d_p	Planet gear diameter
d_{rg}	Ring gear diameter
K_r	Scaling factor
T_m	Gearbox output shaft torque
K_{ag}	Application factor
K_f	Tooth loads intensity index
W_c	Gearbox weight constant
u	Gearbox ratio
u_s	Planetary gearbox ratio
u_{sn}	Gear ratio between sun and planet gears
Z	Planet gears number
T_p	Output torque of the parallel shaft gearbox
T_p	Output torque of the planetary gearbox
c_{gear}	Gearbox specific cost
G_{gear}	Gearbox weight
C_{gear}	Gearbox estimated cost
p_{gear}	Gearbox losses
k_g	Speed-dependent losses constant
P_N	Tidal stream turbine rated power
n_r	Rotor speed
n_{r_N}	Rated rotor speed
T_{EM}	Electromagnetic torque
A_L	Stator current loading
$B_{g_{max}}$	Maximum air-gap flux density
B_g	Air-gap flux density
B_{max}	Saturation flux density
k_{b1}	First harmonic winding factor

ψ	Phase shift between the electromotive force and the current
R_s	Stator radius
R_i	Internal generator radius
R_e	External generator radius
L_m	Equivalent core length
k_D	Air-gap coefficient
h_g	Mechanical air-gap
$h_{g'}$	Additional Carter air-gap
k_c	Carter factor
h_m	Magnet height
μ_0	Vacuum permeability constant
μ_{rm}	Magnets relative permeability
B_r	Magnets remanent flux density
$B_{g_{max}}$	Maximum air-gap flow density
τ	Pole pitch
h_{ys}	Stator yoke height
h_{yr}	Rotor yoke height
h_s	Slot height
k_f	Fill factor
β_t	Teeth pitch ratio
w_t	Stator tooth width
p	Pole pairs number
S_{pp}	Slots per pole per phase number
m	Phases number
H_{max}	Maximum magnetic field in the magnet
H_{cj}	Permanent magnet coercive magnetic field
p_{Fe}	Iron losses
f_e	Magnetic field frequency in the iron

p_{Fe0h}	Specific hysteresis loss
p_{Fe0e}	Specific eddy current loss
N_s	Phase winding number of turns
L_{sl}	Leakage inductance
L_{slot}	Slot leakage inductance
L_{end}	End winding leakage inductance
C_{conv}	Power electronics cost
C_g	Permanent magnet generator cost
C_{TST}	Tidal stream turbine cost
c_{Cu}	Copper specific costs
c_{Fe}	Iron specific costs
c_m	Permanent magnet specific costs
G_{Cu}	Copper weight
G_{Fe}	Iron weight
G_m	Permanent magnet weight
f_{max}	Maximum electrical frequency

1. Introduction

1.1 Overview

Tidal energy is due to oceanic tides, which are periodic and depends on the gravitational attraction exerted by the moon. Such phenomena creates strong current forces which can be harnessed and converted to electricity by means of tidal stream turbine generators. These properties make the tidal stream energy advantageous over wind or solar energy in terms of predictability and power density. Indeed, many tidal stream turbines systems were employed last decade. Among them, some industrial tidal power schemes are cited below:

- In the Race Rocks Demonstration Project, a tidal stream turbine demonstration was installed at Race Rocks (Canada) in 2006. The project is shut down in 2011 because of the high operating cost.
- Jindo Uldolmok Tidal Power Plant in South Korea in 2009.
- The 1.2 MW SeaGen tidal turbine in Strangford (United Kingdom) in 2008.
- The 500 kW OpneHydro/Naval Group direct-drive tidal stream turbine in France.
- The 1 MW Andritz/Hammerfest tidal stream turbine in Okney Islands (United Kingdom).
- The 1 MW Alstom tidal strem turbine in Orkney Islands (United Kingdom).
- The 1 MW voith Hydro tidal stream turbine in the island of Eday (United Kingdom).

Despite the technological advancement in tidal stream energy production, many technical and economical issues was encountered, which discourage the investment in such domain. Indeed, the tidal turbine technology is at its infancy and need more research and development.

1.2 Issues and challenges

The tidal current energy production suffers from many problems which can be summarized in two axes: 1. Cost-effectiveness. 2. Bio fooling and environmental issues. The cost-effectiveness issues is related to the techno-economical ones. Whereas, bio fooling and environmental problems concerns the sea life that can affect or be affected by the marine generators.

1.2.1 Cost-effectiveness

Tidal energy projects require an expensive initial budget which make such energy unpopular. Moreover, tidal stream turbines are based on new technologies, where new drivetrains and generator topologies are employed. Therefore, more investigations are required to choose the good configuration options to employ. On the other hand, the cost can be improved by choosing the relevant deployment sites, where further investigations are needed in this topic. Therefore, cost-effectiveness can be improved by:

- Improving the system availability and reliability.
- Enhancing existing technologies already developed in similar systems such wind turbines.
- Developing new reliable technologies as magnetic gearing.

1.2.2 Biofouling

Unlike wind turbines, tidal turbines are submarine systems, which suffer from the biological fouling (biofouling). Biofouling is a biological phenomena that happens when any structure is placed in high tides levels sites. Such problem reduces the hydrodynamic efficiency of blades, which causes high power losses, the need of regular cleaning, and the the operating cost increase.

1.2.3 Environmental concerns

Tidal stream turbine affects the sea wild life with their emitted noise. The rotating blades kill accidentally swimming sea animals. Even if a safety mechanism is employed to turn off the turbine, the sea animals can cause a huge loss of energy during the cut-out period. In addition to the lubricating oil impact on the sea water animals, the painting used to prevent the biofouling growth can be harmful to them.

1.3 Thesis outline

As previously presented, the tidal stream energy production suffers from many issues. In this PhD thesis, the availability and reliability of tidal stream turbines is investigated according to their drivetrain configuration and basing mostly on wind turbines reliability data. Besides that, the cost-effectiveness of the mainly employed drivetrain options in the tidal turbine systems are investigated, where the Ouessant site marine energy potential is considered. In addition, magnetically gearbox driven generator is proposed as a promising technology in the field of marine energy production. It is afterwards designed and optimized considering tidal turbines specifications.

The thesis content is structured in four chapters:

- Chapter 2 deals with the tidal stream turbine availability and performance according to the drivetrain option. In this context, a review-based comparative study is performed to investigate the suitable drivetrain option for tidal stream turbine applications. The study focuses on the presence or not of a gearbox in the drivetrain and its impacts on the overall system availability and performance.
- Chapter 3 is devoted to the design modeling of the two-stage gearbox driven tidal stream turbines, the single-stage gearbox driven one, and the direct-driven one. First, the model of the marine current resources, where the turbine is supposed to be installed, is taken in consideration. The model allows the calculation of annual harnessed energy depending on the power rating, the cut-in speed of the generator, and the hydrodynamic efficiency of the turning blades. Secondly, an analytical design model of two types of gearboxes (parallel shaft, planetary) is developed by considering the tidal stream turbine specifications. Lastly, a two-dimensional analytical model based on magnetic circuit calculation is adopted for the permanent magnets generator sizing.
- In chapter 4, the design optimization of the tidal stream turbine is performed. Indeed, three drivetrain configurations are considered: the single-stage gearbox driven tidal stream turbine, the two-stage gearbox drive one, and the direct-drive one. The estimated cost and size of the three designed systems are compared. Besides, the gearbox ratio impact and cost-effectiveness are investigated by considering different power ratings.
- Chapter 5 deals with the finite element based design optimization of a $500kW$ magnetically-geared generator for tidal stream turbine applications. Such generator topology is proposed in chapter 2 as an alternative solution due to its technical advantages. Fist, the pseudo-direct drive, which is an outer-stator

magnetically-geared generator, is introduced as well as its operating principles. Than, an analytical rough design is developed to be used as an initial sizing model. The Design optimization methodology is afterwards presented, where the feasible direction method is adopted as an optimization algorithm.

2. Tidal Stream Turbine Drivetrain Configurations

2.1 Background

Tidal stream energy is acquiring more attention as a promising renewable energy source. Tidal current oscillations are highly predictable unlike solar or wind energy. Tidal stream turbines, which are analogous to wind turbines, convert the marine current energy to electrical one. However, tidal stream turbine technology is still in development stages contrary to wind turbine technology. Besides that, tidal stream turbines are submerged systems, which increases their criticality due to the submarine aggressive environment. Therefore, tidal stream turbines are potentially exposed to high downtimes due to the difficulty to access to the submerged system. For these concerns, tidal stream energy is considered as an expensive one and to make such energy competitive and largely deployable many improvement need to be addressed. Indeed, many prototypes were created last decades, where many concepts are competing for supremacy.

According to the drivetrain and generator topology, tidal stream turbines can be divided into two mean types:

- Gearbox driven tidal stream turbines with high speed generators.
- Direct drive tidal stream turbines with low speed generators (without a gearbox).

Drivetrain and generator configuration choices present one of the most important concerns for tidal stream turbine industry (as it is for wind turbine industry), where the main problematic is: should gearboxes be used or not. Indeed, the tidal stream turbine configuration choices affect the availability and the cost of energy. However, tidal stream turbine industry is in its early stages and the reliability data of these systems are rare. Hence, to advance the tidal stream turbine technologies development, knowledge and know-how acquired last decades on wind turbines could be transferred.

Since 1991, direct-drive concept appears in wind turbine industry to minimize maintenance problems and avoid mechanical gearbox failures. This option has been adopted by OpenHydro/Naval Energies in their tidal stream turbine (fig. 2.1).

FIGURE 2.1: OpenHydro/Naval Energies direct-drive tidal stream turbine [1].

Although direct-drive systems are efficient and reliable, their high cost and high weight have hindered their widespread deploy. Besides that, mechanical gearboxes used in geared tidal stream turbines are a mature standardized technology and their reliability is improving [3]. Indeed, geared tidal stream turbines have been adopted in well-known tidal turbine projects (fig. 2.2) [1]. However, the mechanical gearbox is still a critical subsystem which requires regular maintenance and has a high mean time to repair especially in the case of submarine systems. It is accordingly clear that both gearbox driven and direct-drive concepts have pros as well as cons and tidal stream turbine industry has not yet converged to one recommended topology. This chapter discusses different drivetrain configurations and compare them qualitatively basing on wind turbine failures data and statistics.

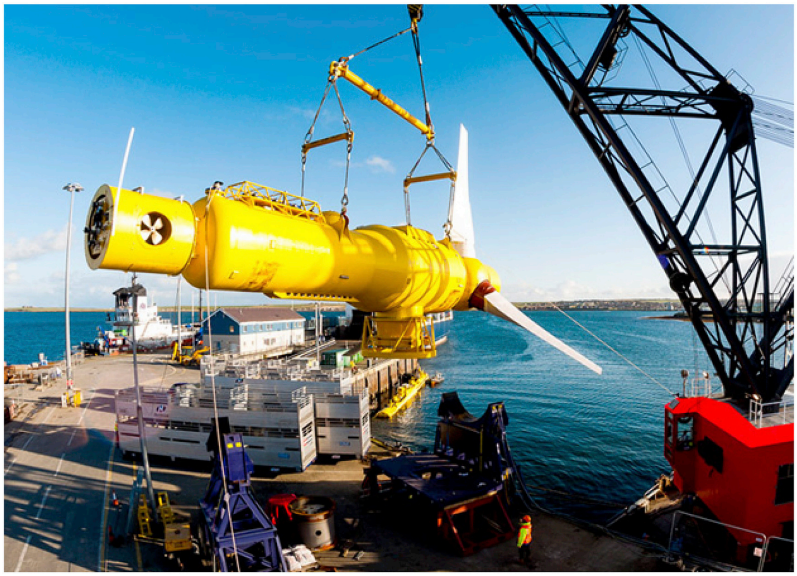

FIGURE 2.2: GE/Alstom geared tidal stream turbine [1].

2.2 Tidal stream turbines drivetrain availability

Tidal stream turbines and wind turbines systems are analogous, which allows to assess their reliability and compares qualitatively between the different existing drivetrain configurations. Although the tidal stream turbine failures data are not available, last years some failures have been reported. The first turbine failure concerns the 1 MW OpenHydro direct-drive tidal stream turbine in Canada (Bay of Fundy) in 2009 (fig. 2.1). The problem have been reported after three weeks of the deployment because of blades failure due to fatigue issues. Another blade fault have been reported at the Atlantis Resources AK1000 tidal stream turbin in 2010 due to manufacturing fault [2]. Therefore, to predict such failures and avoid long downtimes a condition monitoring scheme is needed [2, 28, 29]. However, condition monitoring for tidal stream turbine should be specific to consider the marine current load variability and amplitude [4, 30]. Indeed, tidal stream turbines input torque is 50% much greater than wind turbines one for the same rated power due to the high water density compared to air [31]. Moreover, it has been shown that the shaft speed variations are greater for tidal stream turbines than for wind turbines even though wind current fluctuations are greater [31]. Accordingly, the high loading torque fluctuations highly affects the reliability of tidal stream turbine mechanical subsystems especially the gearbox. In the study [2], tidal turbine components criticality are evaluated according to their Risk Priority Number (RPN) (see equation (2.1)), which is the multiplication of occurrence (O_{cc}), severity (S_v), and probability of failure detection (P_f) [32].

$$RPN = O_{cc} S_v P_f \tag{2.1}$$

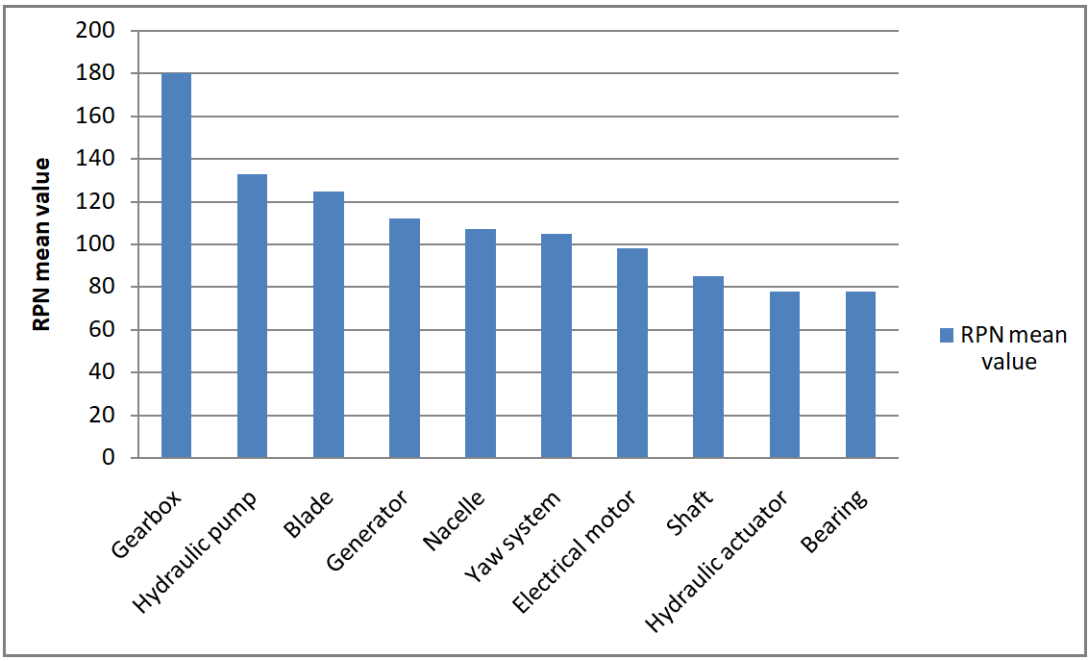

FIGURE 2.3: Tidal turbine sub-assemblies criticality [2].

Figure 2.3 shows that the gearbox has the highest RPN. As for wind turbines failures survey [3, 33], it has been shown that the gearbox downtime is relatively high when compared to the other subsystems. Hence, higher gearbox downtimes will be experienced due to the difficulty to access along with the weather conditions [34].

2.3 Geared vs. gearless tidal turbine : progress on both sides

2.3.1 Gearbox and geared turbines

Last decades, gearbox failures affected the wind turbine industry through downtime and cost of repair (fig. 2.4). However, geared systems components, especially the generator, are standardized, available in the market, and cheaper [35]. Moreover, geared wind turbines are widely deployed during last decades which offers a large theoretical and practical knowledge. Such knowledge presents a great advantage to accelerate geared tidal turbines development [36]. Gearboxes, as a mature technology, are widely used in transport, energy, and process industries. They are vital

components and their mean time to repair (MTTR) is usually the highest among the other subsystems.

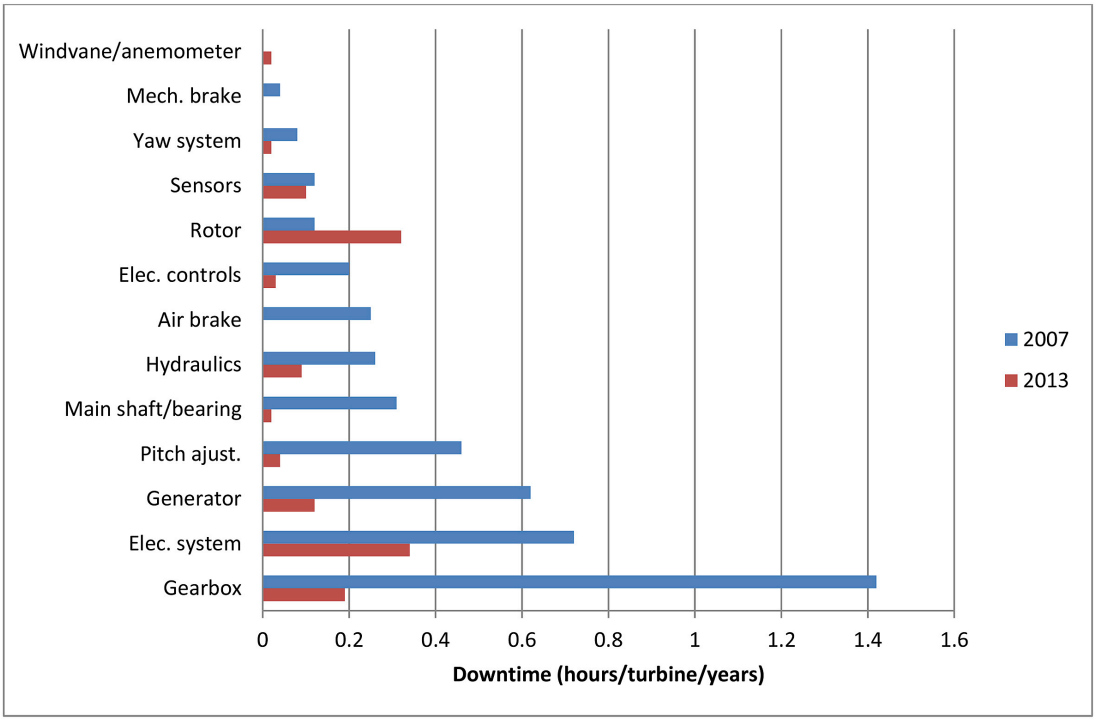

FIGURE 2.4: Wind turbine subsystems downtime [3, 4].

The availability of wind turbine gearboxes, based on the National Renewable Energy Laboratory reliability database, has been improved from 2013 [3]. Such improvements can be qualitatively considered although the logistic delay time and MTTR of offshore tidal stream turbines are higher than onshore wind turbines, mainly due to the difficulty of on-site access. Concerning the gearbox failures rate, it is less than 15%, of which 76% are due to bearing faults, however electrical sub-assemblies faults are more than 25% [37, 38].

Besides that, Energiforsk has led an important project in 2016, entitled "Maintenance effect on present and future wind turbine gearboxes" [5]. In this project, the reliability of three types of gearboxes under different conditions have been analyzed. The objective was to improve wind turbine gearboxes reliability by identifying optimal maintenance schedules and improving gearbox designs. The project studied three (2 MW) wind turbine gearboxes: A typical 3-stage gearbox (fig. 2.5) [29], an optimized design of the typical gearbox, and a future gearbox design. The main obtained results show that the typical gearbox and the optimized one become less reliable if conditions change (application factors), whereas the future gearbox design remains unaffected. Accordingly, in addition to condition monitoring, advancements

in optimization present an important factor to improve gearboxes reliability whatever the industrial application.

Regarding the development of tidal stream turbine in this field, fig.2.6 illustrates some important projects dealing with geared systems [1, 6], while fig. 2.7 presents some commercialized tidal stream gearboxes [7].

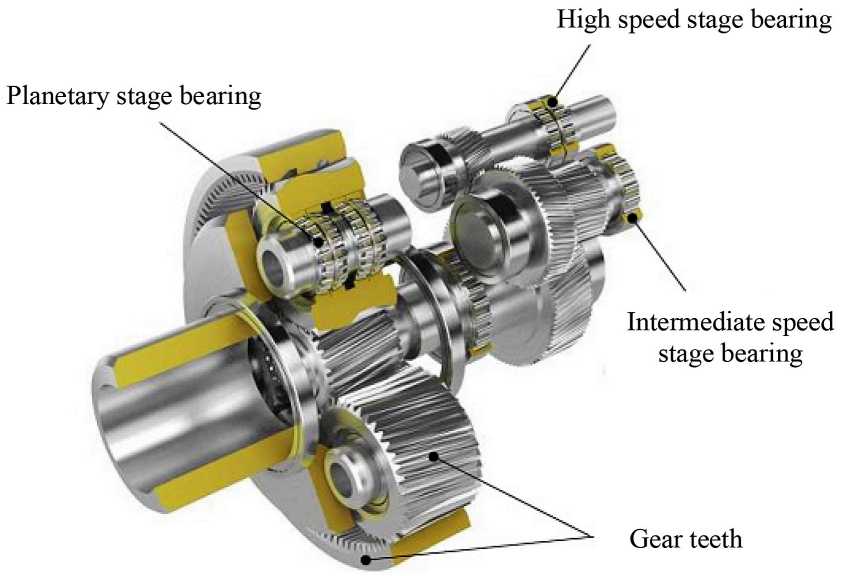

FIGURE 2.5: Typical planetary gearbox [5].

2.3.2 Gearbox issues mitigation

Typical operations and maintenance actions, such as the fine filtration of lubricating oil and the use of remote condition monitoring, are required to detect incipient faults and ensure the good functioning of gearboxes particularly in offshore applications [39]. Besides that, manufacturers try to prolong the service life of wind turbines by developing more robust gearbox systems that withstand the varying load torque. In this context, the Pure Torque concept is proposed by GE/Alstom [8]. In fact, in addition to the rotational forces, wind turbine rotor transmits side forces to the main shaft and gearbox due to the high load input. In the Pure Torque design, a cast iron frame supports the rotor shaft as an extension of the tower structure (fig. 2.8). Hence, the deflective loads are diverted to the front frame not to the drivetrain. Moreover, even under extreme load cases, gearbox misalignment and displacements stay steady with low amplitudes. On the other hand, according to an Alstom study covering 930 wind turbines with rated power from 1.67 MW to 3.0 MW and during 5.5 years, gearbox failure rate causing replacements was lower one order of magnitude than in other drivetrain configurations. This concept is chosen to design the offshore wind turbine GE/Alstom 6MW Haliade 150 (fig. 2.9) [8, 9, 40, 41].

(a)

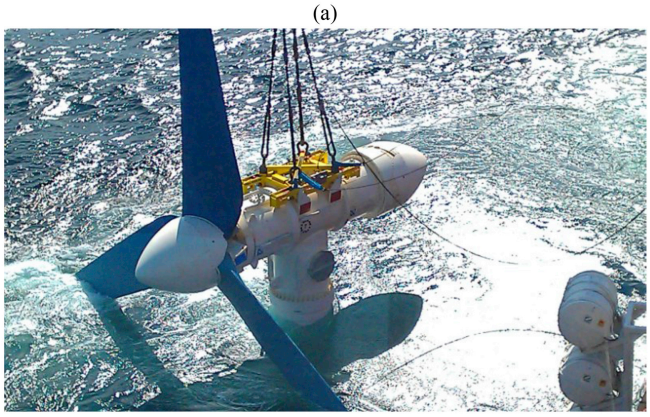

(b)

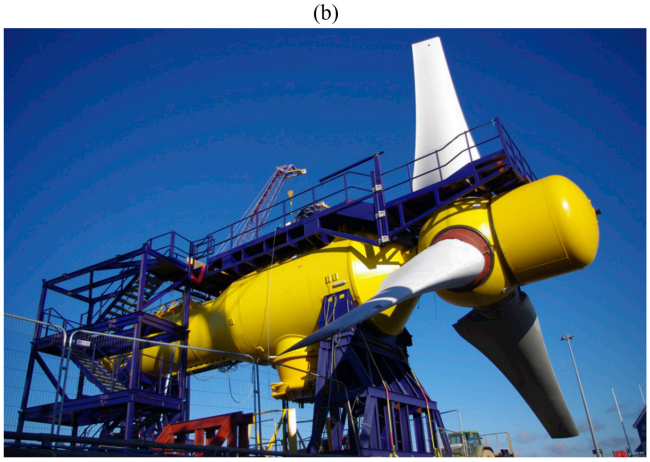

(c)

FIGURE 2.6: Geared tidal stream turbines. (a) SeaGen tidal stream turbine (©Simec Atlantis Energy) [6]. (b) AR1000 tidal stream turbine (©Simec Atlantis Energy) [6]. (c) Oceade tidal stream turbine (©GE/Alstom) [1].

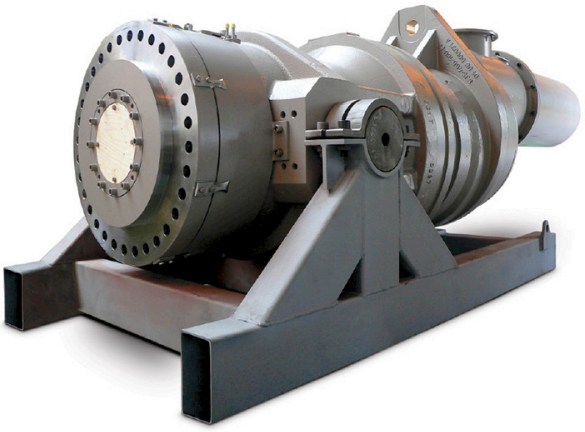

(a) 650kW planetary gearbox with generator of the MCT SeaGen tidal stream turbine.

(b) 1.5MW planetary gearbox of the MeyGen project.

(c) 500kW planetary gearbox of the TGL EMEC demonstrator project.

FIGURE 2.7: Industrial tidal stream turbine gearboxes (©Wikov) [7]. (a) 650 kW planetary gearbox with generator of the MCT SeaGen tidal stream turbine. (b) 1.5 MW planetary gearbox of the MeyGen project. (c) 500 kW planetary gearbox of the TGL EMEC demonstrator project.

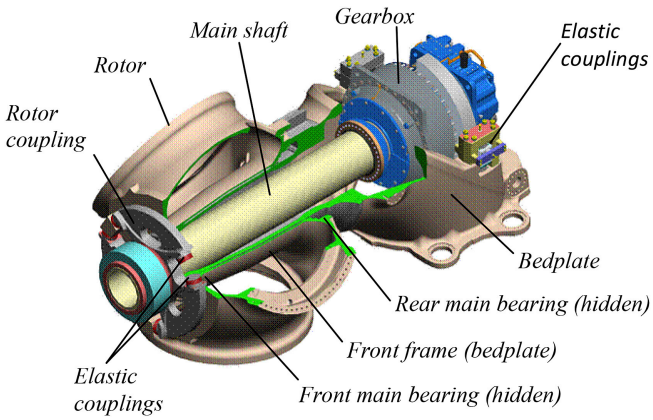

FIGURE 2.8: The Pure Torque concept design [8].

FIGURE 2.9: GE/Alstom 6 MW Haliade 150 offshore wind turbine [9].

2.3.3 Direct-drive turbines

Direct-drive concept is particularly designed to improve reliability by removing the gearbox which is considered as a critical component. In this option, the generator is a low speed and high torque multi-pole one, it has a high diameter, and its mass is therefore considerably high. With the decreasing prices of permanent magnets, the direct-drive systems design moves from wounded rotors to permanent magnet ones which reduces their cost, size, and weight [42]. The direct-drive wind turbines success (e.g. Enercon and Siemens) has proved the commercial viability of unconventional drivetrain options. Therefore, direct-drive configuration have been chosen by many manufacturers for their product [43]. However, the great size and weight due to the generator present a major disadvantage in particular to tidal stream turbines [44]. In fig. 2.10, illustrative examples of such generators are presented [10, 11].

(a)

(b)

FIGURE 2.10: Direct-drive wind turbine generators illustration. (a) Siemens permanent magnet 3 MW, 17 rpm generator [10]. (b) Enercon E-126 7.5 MW, 13 rpm excited synchronous generator [11].

Concerning tidal stream turbines, the direct-drive concept has been approached in both academia and in some important industrial projects [45–50]. In these studies, specific permanent magnet generators topologies have been dealt for tidal stream turbine applications.

The rim-driven concept is part of direct-drive drivetrain options, which is similar to OpenHydro concept (fig. 2.1) [51, 52]. In rim-driven topology (figs.2.11 and 2.12), the generator is inserted in a nacelle in the turbine periphery which is advantageous

in terms of hydrodynamic efficiency compared to POD topology [44]. Despite the encouraging results obtained with this topology, it is still suffering from the considerable weight due to the structural large diameter [53]. Some important projects dealing with direct-drive systems are illustrated in Figure 2.13, [1], [54].

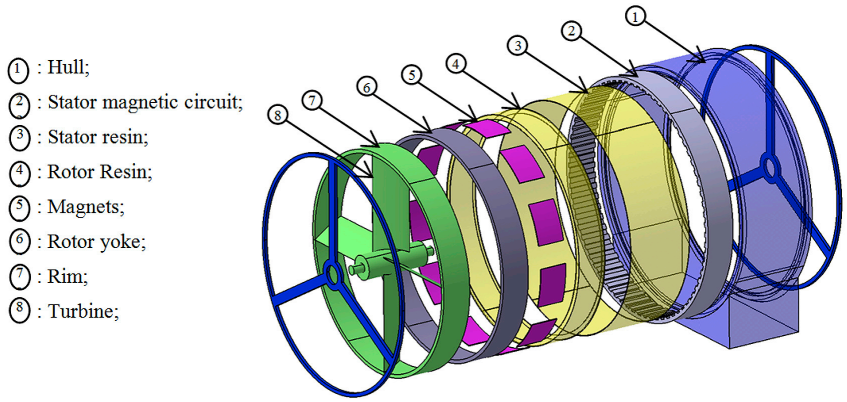

FIGURE 2.11: Rim-driven concept using a radial flux permanent generator [12].

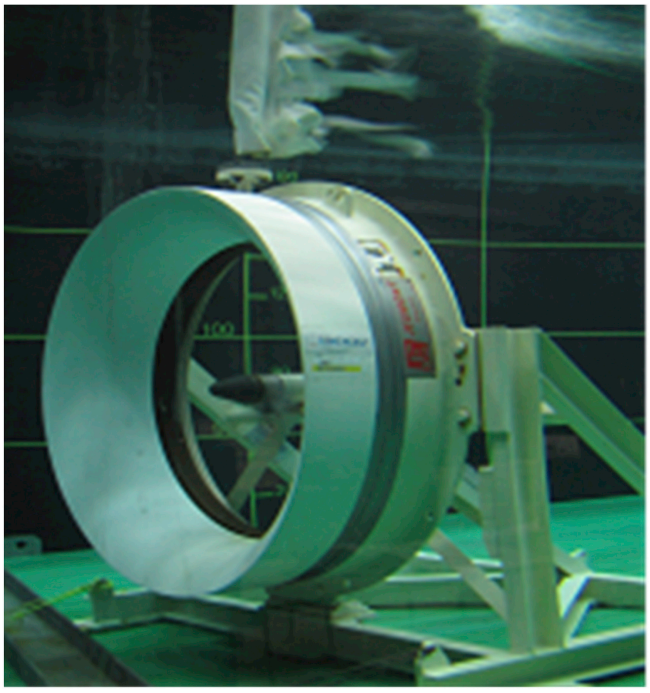

FIGURE 2.12: Rim-driven demonstrator that uses a RFPM generator [12]

(a)

(b)

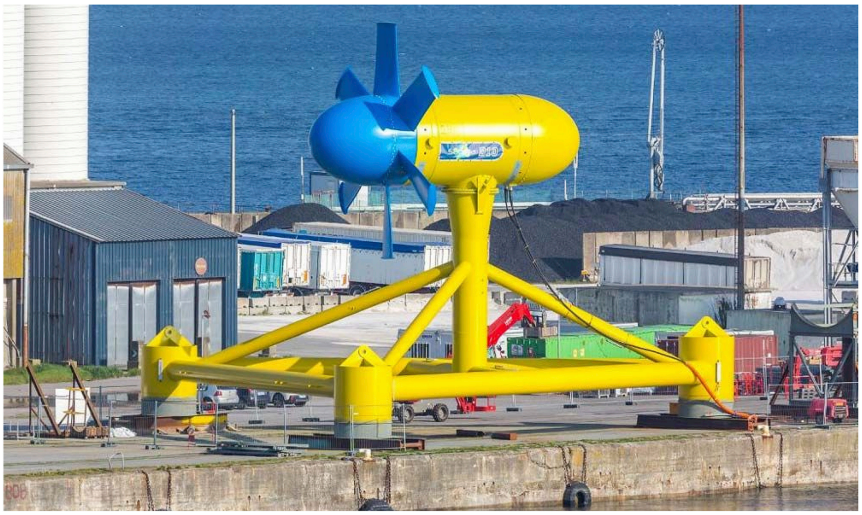

(c)

FIGURE 2.13: Direct-drive tidal stream turbines. (a) OpenHydro Naval Energies tidal stream turbine (OpenHydro). (b) Voith Hydro tidal stream turbine (Voith) [13]. (c) Sabella D10 tidal stream turbine [14]

2.3.4 Integrated drivetrain options : Multibrid

The Multibrid concept is an integrated drivetrain option which is the intermediate between the conventional geared concept and the direct-drive one avoiding their extreme characteristics. In this hybrid solution, the single-stage planetary gearbox (sometimes two-stages), the medium speed permanent magnet generator, the main shaft, and the shaft bearing are all integrated in the same housing. In this case both the generator and the gearbox have approximately the same size which leads to more balanced drivetrain arrangement. This technology, also known as semi direct-drive, was first introduced by AREVA Wind (figs. 2.14 and 2.15) [39, 55, 56].

FIGURE 2.14: View of the Areva Multibrid M5000 wind turbine with 2-stage gearbox (Areva) [15].

FIGURE 2.15: The Areva Multibrid M5000 5 MW wind turbine nacelle (Areva) [11].

A small scale tidal stream turbine system with the same technology have been designed, realized, and tested in the Chinese Zhoushan water channel (fig. 2.16) [16]. In addition to cost and size advantages of Multibrid drivetrain, a recent survey study in the Chinese wind turbine market shows its high availability and operating reliability [17]. In this context, the Chinese Wind Energy Association (CWEA) have conducted an investigation on 47 Chinese wind turbine manufacturers, components suppliers, and developers and results show that the Multibrid wind turbines have the highest annual availability compared to wind turbines with a doubly-fed induction generator (DFIG) or a direct-drive permanent magnet synchronous generator (PMSG) (fig. 2.17).

FIGURE 2.16: Small scale Multibrid tidal stream turbine [16].

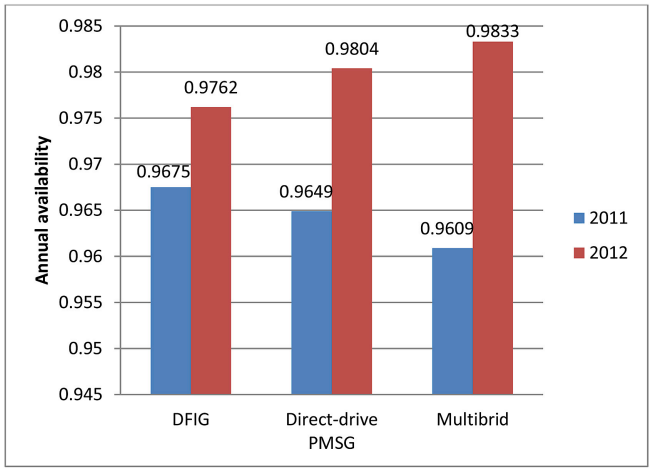

FIGURE 2.17: Annual availability of three wind turbine types in China [17]

2.3.5 Hydraulic transmission

Professor Stephan Salter and his research group at the Endinburgh University for wave energy conversion applications developed a hydraulic transmission based on the Digital Displacement technology (fig. 2.18) [18, 57]. Such transmission can convert a variable low speed high torque input into a constant high speed low torque output. Now, it is commercialized by Mitsubishi Heavy Industries. In 2014, a 7 MW offshore wind turbine demonstration has been planted in Hunterston (Scotland) [58]. Besides that, the authors in [19, 59] investigated the hydraulic transmission where a small-scale tidal stream turbine has been designed and tested (fig. 2.19). Their main results show that the hydraulic transmission option is low efficient compared to the gearbox transmission.

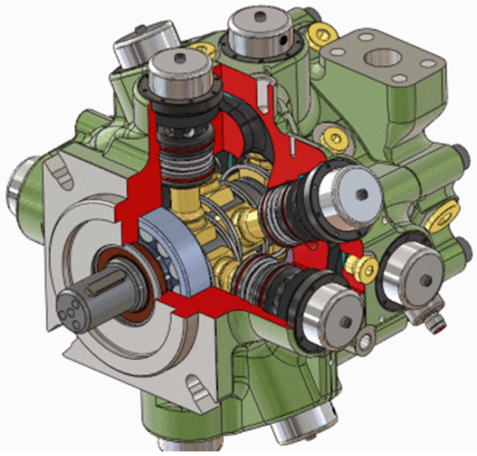

FIGURE 2.18: Digital Displacement hydraulic transmission (©Artemis Intelligent Power Ltd) [18].

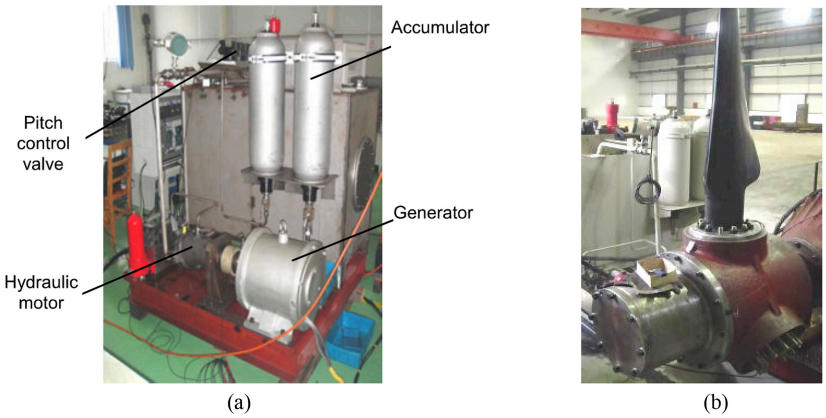

FIGURE 2.19: Tidal stream turbine using a hydraulic transmission system [19]. (a) Hydraulic system. (b) The turbine.

2.4 Geared vs. gearless tidal turbine: performances

Mechanical gearboxes consist of a number of gear stages. In general, three-stage gearboxes are common in the tidal and wind turbine industry but two- and single-stage gearboxes are acquiring more attention as designers try to reduce weight, size, and maintenance costs by using lower speed generators. In [60] it was shown that single-stage gearboxes, with a low gear ratio, can be the most efficient. Besides that, the generator design and topology differs depending on the chosen drivetrain configuration and the number of stages if the gearbox exists. The performances of each configuration are discussed and compared in [35, 61–63].

For instance Tavner et al. [64,65] investigates the reliability of wind turbine generators and converters. The obtained results show that the direct-drive wounded rotor synchronous generators (WRSG) failure rates are more than the double of those geared generators. Moreover, converter and electronics failures rate of direct-drive wind turbines are considerably higher compared to geared ones. Indeed, the paid price to improve the direct-drive wind turbines reliability, by removing the gearbox, has led to a decline of electrical parts reliability. However, due to the long downtime of mechanical gearboxes compared to electronics and converter components, the gearbox driven wind turbines were less available. Accordingly, direct-drive WRSG appears not suitable for tidal stream turbine applications in particular for high power rating.

In another paper [66], a techno-economic study have been carried out to compare the operational aspects of direct-drive and geared onshore wind turbines. This study shows that the geared concept remains being preferable from the economical viewpoint, and to make direct-drive concept cost competitive, its components costs should be reduced by 50%.

The authors in [60] investigate the cost of energy and performances of four generator topologies: the direct-drive permanent magnet generator (DDPMG), the permanent magnet generator with a single-stage gearbox (PMG1G), the permanent magnet generator with a two-stage gearbox (PMG2G), the permanent magnet generator with a three-stage gearbox (PMG3G). The study considers typical 6 MW offshore wind turbines and the results show that the DDPMGs have significant copper losses (almost half the total losses) due to the high number of coils in such topology. Besides that, the availability is high despite the high winding faults.

Concerning the PMG1G configuration, the generator is smaller and lighter compared to direct-drive one due to its low torque rating. In addition, the single-stage gearbox is more efficient than the other gearbox types. The PMG1G converter losses are relatively similar to DDPMG ones. However, compared to PMG2G and PMG3G, the

PMG1G is also advantageous due to its balanced gear, iron, and copper losses. Regarding the availability the PMG1G is competitive to DDPMG despite the mechanical failure due to the gearbox.

The PMG2G is considerably smaller than the previous generators, but the additional gear stage leads to more gear losses and increases the size, weight, and cost of the gearbox.

Even if the three-stage gearbox driven generator is not recommended for tidal stream turbine applications, the generator is more compact, more efficient, and cheaper. However, the three-stage gearbox have a bigger size and weight and it is more expensive and less reliable.

Concerning the estimated cost of energy, the DDPMG have the lower cost of energy, However this configuration is more sensitive to permanent magnet prices than PMG1G one. An increase of permanent magnet prices scenario can make the PMG1G more advantageous [60].

In Polinder et al. work [35], which precedes the above-cited study, a comparaison between five generator topologies were presented: a doubly-fed induction generator with three-stage gearbox (DFIG3G), a direct-drive wounded rotor synchronous generator (DDSG), a direct-drive permanent magnet generator (DDPMG), a single-stage gearbox driven permanent magnet generator (PMG1G), and a doubly-fed induction generator with a single-stage gearbox (DFIG1G). Similar conclusions were attained where the crucial importance of availability and reliability were highlighted especially in offshore conditions. Another study [20] considered the availability of the following generator topologies: permanent magnet synchronous generator (PMSG), wounded rotor synchronous generator (WRSG), squirrel cage induction generator (SCIG), wounded rotor, and brushless doubly-fed induction generator (DFIG). The comparison results show how promising are single-stage gearboxes even though the direct-drive PMSGs have the lead (fig. 2.20). In this context, direct-drive concept remain being chosen by some wind and tidal turbine manufacturers and developers. Figures 2.21 and 2.22 give an illustrate of recent projects: The coming GE Haliade-X 12 MW wind turbine [21] and the Nova Innovation Ltd D2T2 direct-drive tidal stream turbine [22].

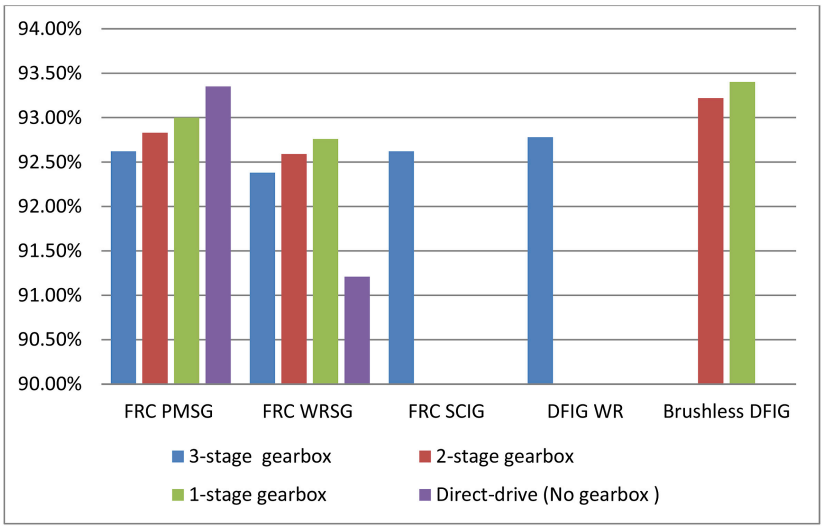

FIGURE 2.20: Drivetrain availability in offshore wind turbines [20].

FIGURE 2.21: Haliade-X 12 MW wind turbine (©GE) [21].

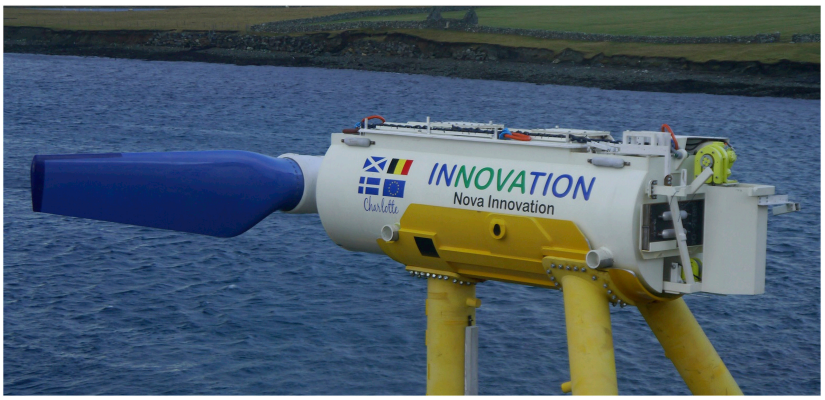

FIGURE 2.22: D2T2 tidal stream turbine (©Nova Innovation) [22].

2.5 Magnetically-geared tidal stream turbines

2.5.1 Magnetic gears

Magnetic gears, which are analogous to mechanical gears, transmit torque from the input shaft to the output shaft by magnetic attraction and repulsive forces between rotating magnets. Contrary to early magnetic gears [67–70], Modern ones have relatively high torque densities compared to mechanical gearboxes which makes them a promising alternative to mechanical gears. Moreover, magnetic gears are based on a contactless transmission of torque which reduces problems related to mechanical gears, such as vibrations, acoustic noise, the lubrication need, and the risk of fatigue and jamming failures [22, 71–75]. Magnetic gears can be classified into three types: the flux-modulated magnetic gear, the harmonic magnetic gear, and the planetary magnetic gear (fig. 2.23) [76]. the flux-modulated magnetic gear , known as the coaxial magnetic gear or the concentric magnetic gear, is the leading design especially when it is integrated with a permanent magnet machine.

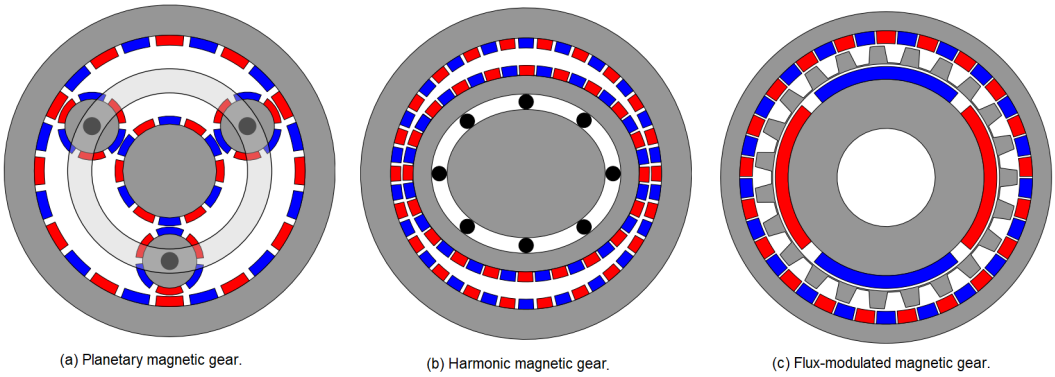

FIGURE 2.23: Magnetic gears main types (MacGilton et al., 2018). (a) Planetary magnetic gear. (b) Harmonic magnetic gear. (c) Flux-modulated magnetic gear.

TABLE 2.1: List of some flux modulated magnetic gear prototypes

Reference	D	G_r	Torque density $[kNm/m^3]$
Atallah et al. [77]	120	5.75	72
Shah et al. [78] (two torque input)	120	5.5/6.5	47/56
Rasmussen et al. [79]	120	5.5	92
Gerber and Wang [80]	150	10.5	62
Frank and Toliyat [81]	120	5.5	42

Table 2.1 shows a list of some flux-modulated magnetic gear prototypes with their diameters D, their gear ratios G_r, and their torque density.

2.5.2 Magnetically-geared tidal stream turbine

Mechanical gearboxes are used to improve the torque density of the couple gearbox-generator which makes such systems compact compared to direct-drive ones. Magnetic gearboxes have the same role if it is cascaded with generator. However, if the generator is magnetically and mechanically integrated with the magnetic gearbox higher torque densities can be achieved. The flux-modulated magnetic gear seems being the suitable design for this kind of integration due to its simplicity and balanced design. Many designs and prototypes proposed and developed for wind turbine applications can be suggested and mirrored for tidal stream turbine systems. Some prototypes of such integrated machines are cited in table 2.2.

TABLE 2.2: List of some flux modulated magnetically-geared machine prototypes

Reference	$D[mm]$	G_r	Torque density $[kNm/m^3]$
Atallah et al. [82]	178	11.5	in excess of 60 (measured)
Jian et al. [24]	194	7.3	87 (simulated)
Rasmussen et al. [83]	268.5	8.83	92 (measured)
Wang et al. [84]	320	6.6	105 (simulated, only the gear)
Johnson et al.(a) [85]	800	11.33	82.8 (measured)
Johnson et al.(b)(axial flux) [86]	280	4.17	94.4 (measured)

Pseudo direct-drive generator

The pseudo direct-drive generator is an outer stator magnetically-geared generator, where the coaxial magnetic gear outer rotor is stationary and fixed to the stator internal bore (fig. 2.24). In this configuration, the modulator is the low speed rotor which could be connected to the tidal stream turbine low speed shaft. In fact, this prototype is a promising compact and efficient alternative solution to avoid the drawbacks of both gearless and geared configurations [25, 82]. Concerning tidal stream applications, Magnomatics and Seaplace worked on a project to develop and test a 1/13 scale pseudo direct-drive tidal stream turbine demonstrator. The generator was short-listed as one of the best projects.

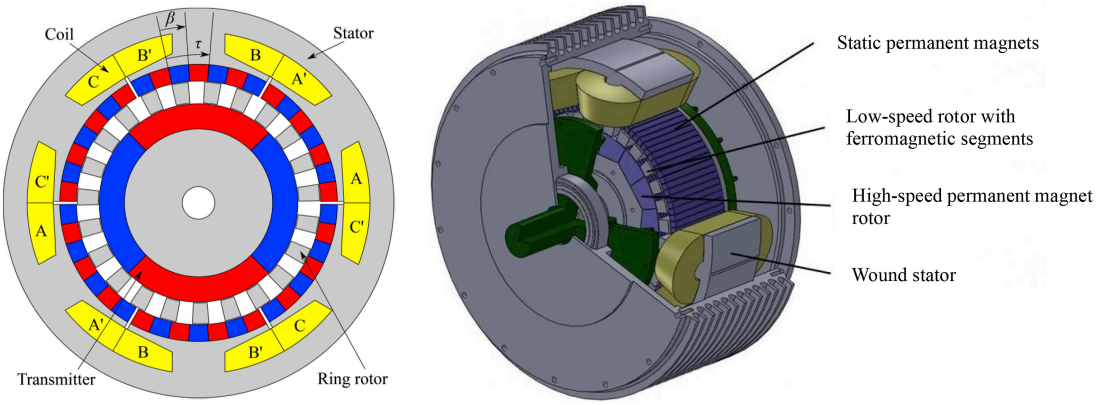

FIGURE 2.24: Scheme and illustration of the pseudo-direct drive generator [23].

Magnetically-geared inner stator permanent magnet generator

This configuration is similar to the last one, however the stator is implemented inside the coaxial magnetic gear. This topology seems to be suitable to wind turbines and can be easily extended tidal stream turbines (fig. 2.25) [24].

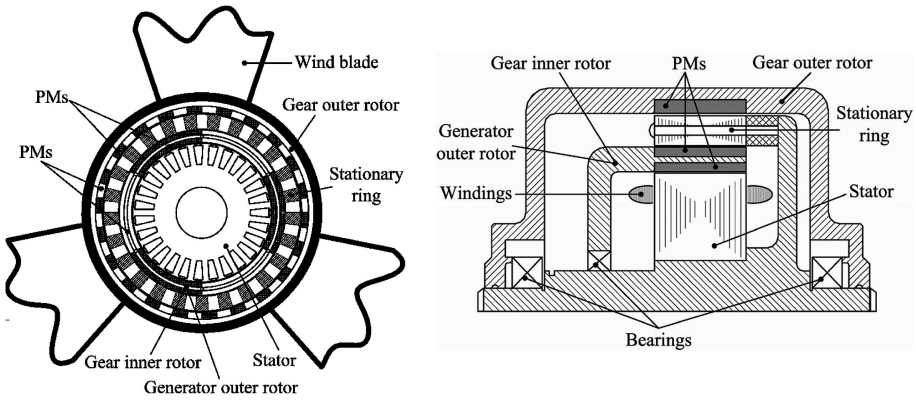

FIGURE 2.25: Magnetic-geared inner stator permanent magnet generator [24].

Axial flux magnetically-geared generator

This generator consists of an axial flux permanent magnet generator integrated in the radial bore of an axial flux magnetic gear (fig. 2.26) [86]. As mentioned in table 2.2, the generator have a torque density of $94.4 kNm/m^3$. Such topology can be chosen for a rim-driven tidal stream turbine with the possibility of using multiple rotors or stators [12].

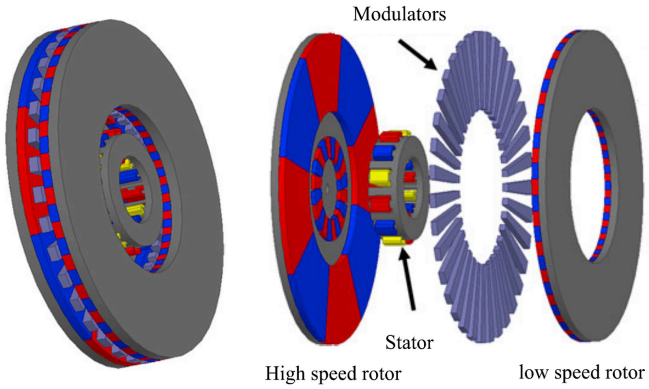

FIGURE 2.26: Axial flux magnetically-geared generator [25].

The previous-presented magnetic gear based topologies present an obvious interest for marine renewable energy harvesting systems, where the high availability is a challenge. Most of the investigations were on wave energy converters where the interest of magnetic gears has been raised [36, 85]. Concerning tidal stream turbines, few papers have been reported. In [78], a magnetic gear prototype has been designed and tested for a contra-rotating tidal stream turbine. Figure 2.27 shows another small-scale magnetically-geared tidal stream turbine which has been successfully designed and realized [26].

2.5.3 Challenges

Magnetic gearboxes can replace mechanical ones especially in wind turbine and tidal turbine industry due to many advantages such as:

- Contactless torque transmission
- High reliability
- Overload protection
- Reduced noise and vibrations
- High efficiency

However, this technology is still in its infancy where some challenges remain. The first challenge concerns the design process of magnetically-geared generators. Indeed, such design consider both the magnetic gear and permanent magnet generator which have to be well matched, coupled, and satisfy the design specifications. The mechanical manufacturing, as another challenge, is more complex then it is in conventional electrical generators. Although the generators based on the coaxial magnetic gear concept are relatively simpler. Besides that, the cost of magnetic gears and generators derived from them is highly sensitive to permanent magnet material prices.

Therefore, the feasibility of such technology depends on the permanent magnets cost and its availability [87].

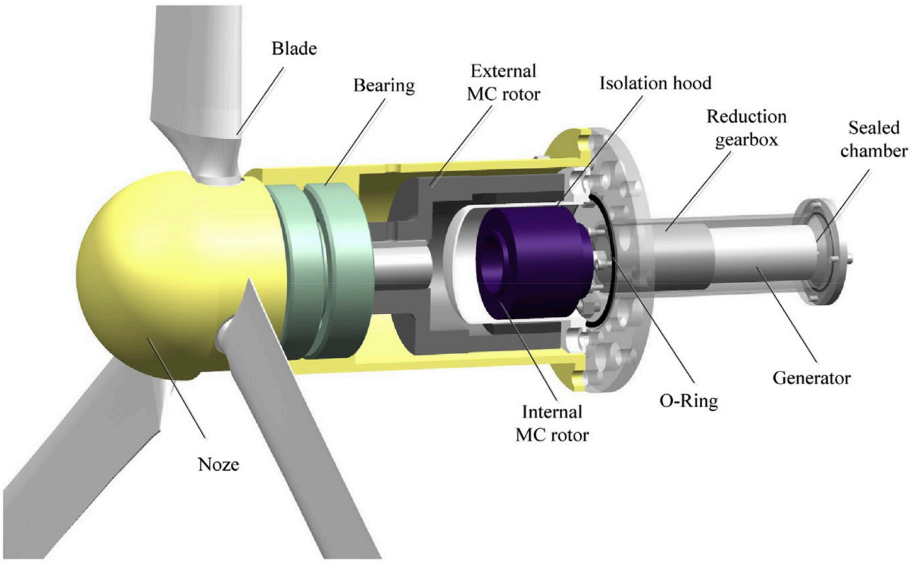

(a)

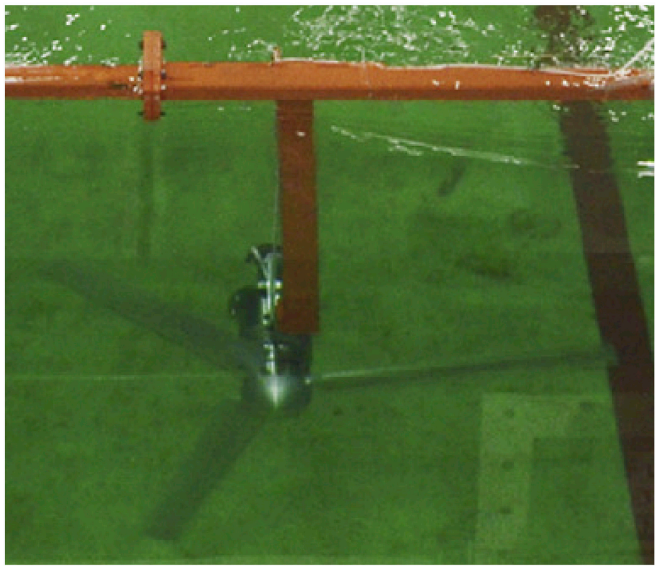

(b)

FIGURE 2.27: Small scale magnetically-geared tidal stream turbine [26]. (a) Tidal stream turbine view. (b) Prototype.

2.6 Comparison summary

The comparative study between the four generator structures: three-stage gearbox driven generator, Multibrid generator, direct-drive generator, magntically geared generator is summarized in Table 2.3:

TABLE 2.3: Drivetrain technologies comparison

Drivetrain concept	Drivetrain technology	Pros and cons
Mechanically geared	3-stage gearbox driven	+ Standardized technology + Commercially available + Relatively cheaper – Low availability – High mechanical losses – No overload protection
	Multibrid (2- & 1-stage gearbox)	+ Compact design + High efficiency + High availability + Reliable and cheaper gearbox – Unconventional concept
Gearless	Direct-drive	+ Concept simplicity (no gearbox) + High availability + Commercial viability – High size and weight – Relatively expensive – High electrical failures rate
	magnetically-geared	+ Compact design + High availability + High efficiency + Overload protection – Technology under development – Dependency to PM prices – Generator complexity

2.7 Conclusions

This chapter has addressed the critical issues which concerns the drivetrain configuration choices, where a review-based investigation and comparison is proposed basing mainly on the wind turbine industry data. the comparative results are discussed below:

- Gearbox technology is mature and widely used in wind turbine industry. such large use leads to more and more improvements especially in terms of reliability.
- Due to its high reliability, the Multibrid concept (single-stage gearbox driven generator) is a promising alternative to conventional configurations even if it is not yet standardized. Further design optimization on such configuration can accelerate its integration into tidal stream turbines.

- Direct-drive concept presents an interesting choice. However, such drivetrain configuration is costly and its manufacture standardization is insufficient. furthermore, the direct-drive generator is too large and it is subject to high failure rate.
- Concerning efficiency, mechanical gearboxes cause additional losses which can result in big economical losses during the tidal stream turbine service life. Therefore, in the long term direct-drive generators can be more cost-effective especially if the permanent magnet prices are stable.
- magnetically-geared turbines represents a promising future alternative to usual geared turbines. Indeed, Magnetic gearboxe advantageous properties as the contactless torque transmission, the high efficiency, and the passive overload protection can replace mechanical gearboxes especially in specific fields where the reliability is important. However, a large deploy of such topology requires more investigations on the economical and technical feasibility especially for off-shore or submarine turbines.

3. Grid-connected tidal stream turbine design

3.1 Introduction

The reliability and performance of different types of drivetrain and generator configurations are presented and compared in chapter 2, where the Multibrid drivetrain is proposed as a hybrid solution between the direct-drive drivetrain and the conventional mechanical drivetrain with three-stage gearboxes [88]. In this chapter, the tidal stream turbine system is analytically modeled in order to be optimally designed in the next chapter 4. The tidal current resource is firstly modeled to estimate the annual produced energy as well as to size roughly the turbine tip blades diameter. Than, the grid-connected tidal stream turbine sub-assemblies, which includes the turbine (blades), the gearbox (if the system is geared), the generator, and the power electronic converter, are considered (fig. 3.1). Each component is discussed and modeled apart considering different mechanical drivetrain types: the direct-drive tidal stream turbine, the single-stage gearbox driven tidal stream turbine, and the two-stage gearbox driven tidal stream turbine.

3.2 Renewable resource and turbine modeling

The Renewable resource modeling is necessary to estimate the energetic potential of a submarine site. The site considered in this thesis is the Fromveur passage near the Ouessant Island in France (fig. 3.2).

The tidal current velocity data was calculated basing on the tide atlas, which is collected by the French navy hydro-graphic and oceanographic service [89–91]. The tidal current velocity amplitude and direction are measured hourly during one year (8760 hour).

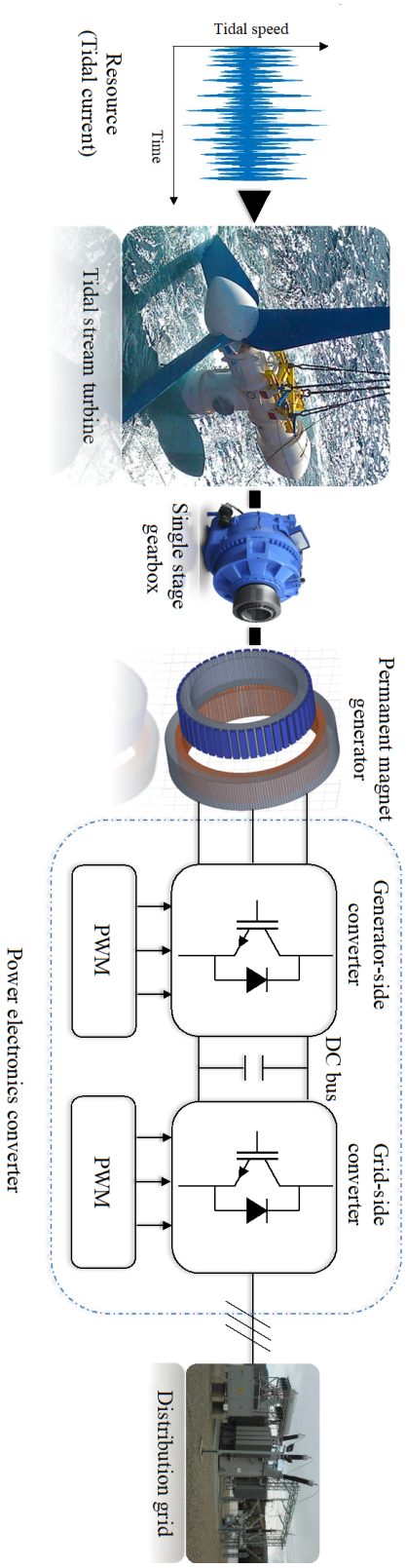

FIGURE 3.1: Scheme of a grid-connected single stage permanent magnet generator-based tidal stream turbine.

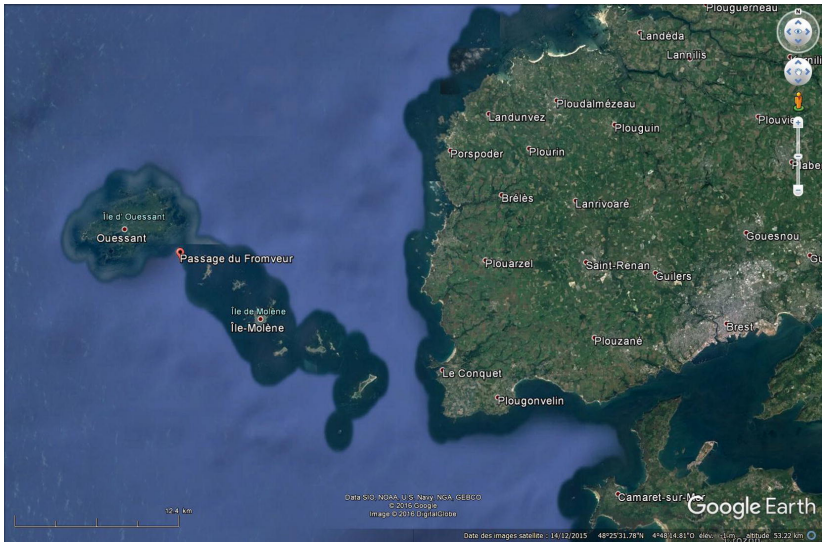

FIGURE 3.2: Fromveur passage (near Ouessant island)

The renewable resource models depend on the site velocity data (speed and angle) and includes the following tidal stream turbine main parameters:

- the cut-in tidal current speed.
- the cut-out tidal current speed.
- the rated tidal turbine power and speed.
- the presence or not of a yaw system.

Indeed, a yaw system is is a component responsible of orienting the tidal stream turbine along the tidal current direction. However, as the tidal stream turbine is a submerged system, the yaw system should be avoided. The alternative solution is to use a bi-directional fixed axis direction tidal turbine. In this case, the turbine axis is fixed along one direction which assures a maximum of produced energy.

3.2.1 Turbine modeling

The turbine blades are modeled by the power coefficient $C_p(\lambda, \beta)$. This coefficient depends usually on two parameters which are the blades pitch angle β and the Tip-Speed Ratio (TSR) λ. The TSR is a ratio between the blades tip speed and the tidal current speed.

$$\lambda = \frac{\Omega_r D_{turbine}}{2v} \tag{3.1}$$

where Ω_r is the rotor rotational speed, $D_{turbine}$ is the turbine diameter and v is the marine current speed. The power coefficient model is based on experimental data

of small-scale blades designed and tested for tidal stream turbine specifications [92]. The power coefficient of such blades are interpolated as Figure 3.3 shows [27].

$$\begin{cases} C_p(\lambda) &= 0.0195\lambda^2(1.3172e^{1.539-0.3958\lambda} - 0.0867\cos(5.6931 - 0.4019\lambda) \\ \lambda &\in [0, 11.8] \end{cases} \tag{3.2}$$

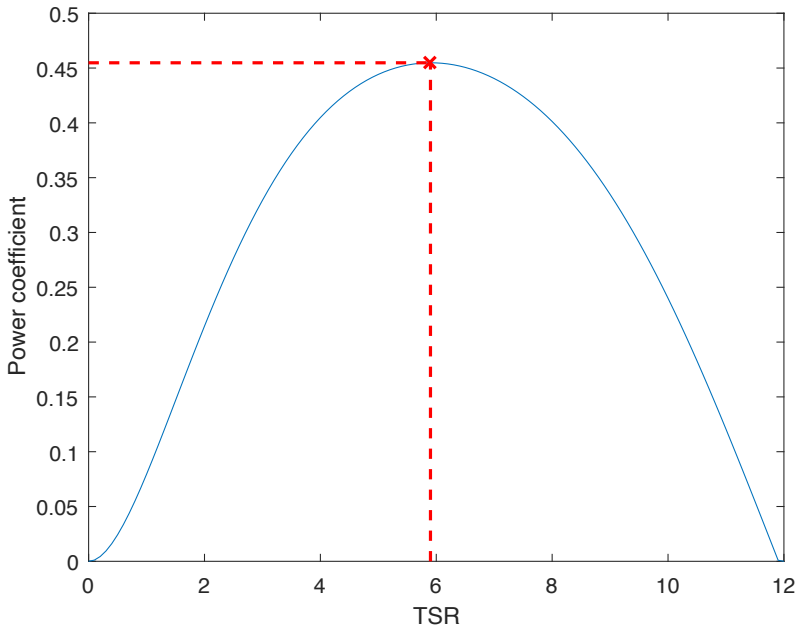

FIGURE 3.3: Power coefficient interpolation.

3.2.2 Annual energy production

Considering the velocity data, the annual energy production (AEP) is the sum of the power during each hour δt (the tidal current speed and power are assumed non-variable) along a year as shown in the following equation.

$$AEP = \sum_{t=1}^{8760} P_T(t)\delta t \tag{3.3}$$

Tidal power P_T of a specific site can be calculated as a function of tidal current speed (velocity amplitude) ($v(t)$) and the turbine rotor diameter (D) as equation (3.4) shows.

$$P_T(t) = \frac{1}{2}\rho C_p(\lambda, \beta) A_t v(t)^3 \tag{3.4}$$

where $A_t = \frac{1}{4}\pi D^2_{turbine}$ is the turbine blade swept area, ρ is the sea water density, $C_p(\lambda, \beta)$ is the power coefficient which characterizes the blades hydrodynamic efficiency.

Regarding the energy, it can be calculated otherwise by considering the speed as a variable in equation (3.4).

$$AEP = \sum_{v \in [v_i, v_n]} P_T(v) OCC(v) dv + P_{Tr} \sum_{v \in [v_n, v_c]} OCC(v) \tag{3.5}$$

Where v_i is the cut-in tidal current speed (turbine starting speed), v_c is the cut-out tidal current speed, v_n is the rated tidal current speed, $P_{Tr} = P_T(v_n)$ is the rated input shaft power which is considered also as the maximum power clipping (power limitation), and $OCC(v)$ function presents the tidal current velocity amplitude distribution. Regarding the power coefficient which characterizes the blades, the maximum is assumed to be maintained during the energy harnessing ($\lambda_{opt} = 5.9$ and $C_{pmax} = 0.4548$). Moreover, the cut-out tidal current speed is taken as the maximum one ($v_c = 6.2m/s$). Regarding the availability, the tidal turbine is assumed available during its service life.

3.2.3 bi-directional fixed axis direction tidal turbine

The tidal stream turbine in this case is fixed along an optimal angle (θ_{opt}. Indeed, the tidal current velocity $v(t)$ at the instant t is composed of an amplitude $v_a(t)$ and an associated angle $\theta_{current}(t)$. Therefore the speed along an angle (θ) is the projection of the velocity on the turbine direction axis.

$$v(t, \theta) = v_a(t) cos(\theta - \theta_{current}(t)) \tag{3.6}$$

Considering equations (3.3) and (3.4), the optimal angle is the one who gives the maximum of produced energy.

$$\theta_{opt} = \underset{\theta \in [-\pi, +\pi]}{argmax}(AEP(\theta)) \tag{3.7}$$

Figure 3.4 illustrate the velocity distribution of the tidal current along polar axis where the optimal direction is presented $\theta_{opt} = 61^o$.

In Figure 3.5, the speed occurrence rate along the considered axis is presented. The same figure can be considered as the probability density of tidal speed currents.

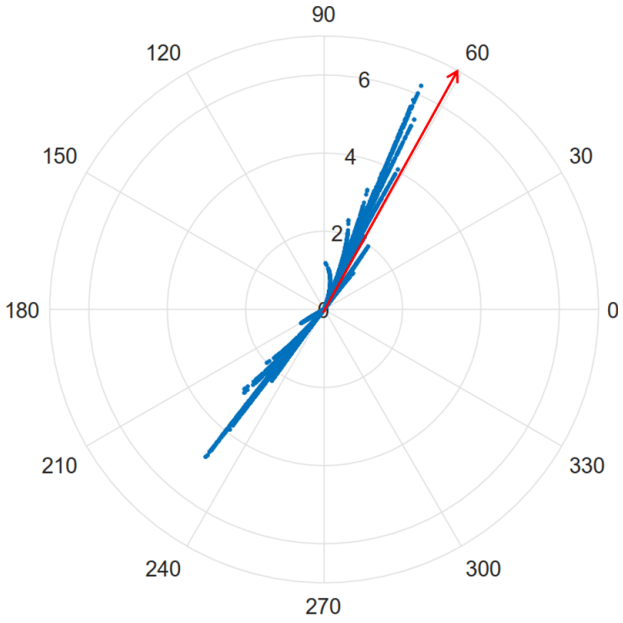

FIGURE 3.4: Tidal velocity in polar coordinates.

Concerning the energy calculation, the swept area is considered equal to $1m^2$. In other words the energy density is calculated instead. Figure 3.6 shows the energy distribution according the current speed.

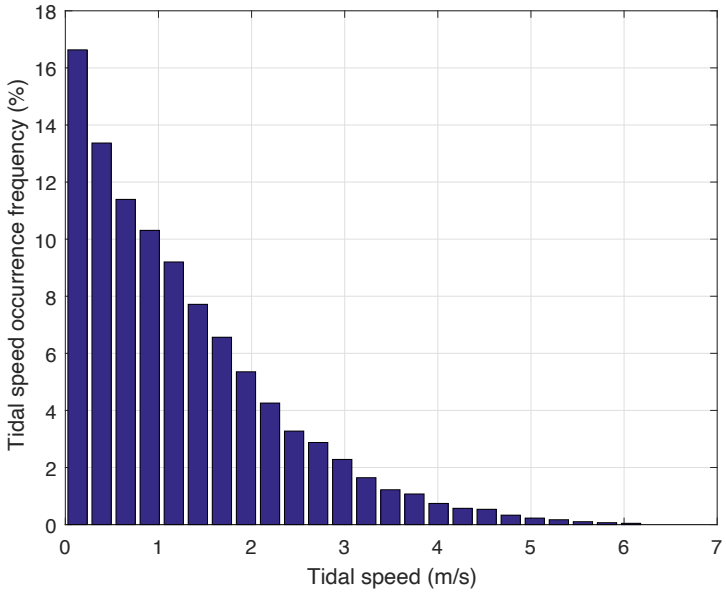

FIGURE 3.5: Tidal current energy distribution along the optimal direction.

The AEP depends on the cut-in tidal current speed and the rated one. Otherwise, it

can be considered as a function of the minimum operating power and the maximum power clipping. This function is illustrated in Figure 3.7.

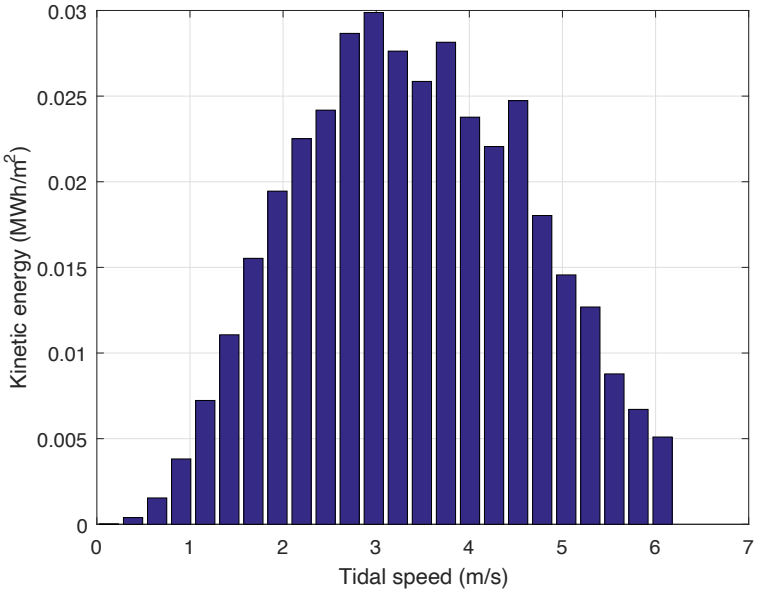

FIGURE 3.6: Tidal current energy distribution (bi-directional fixed axis direction tidal turbine).

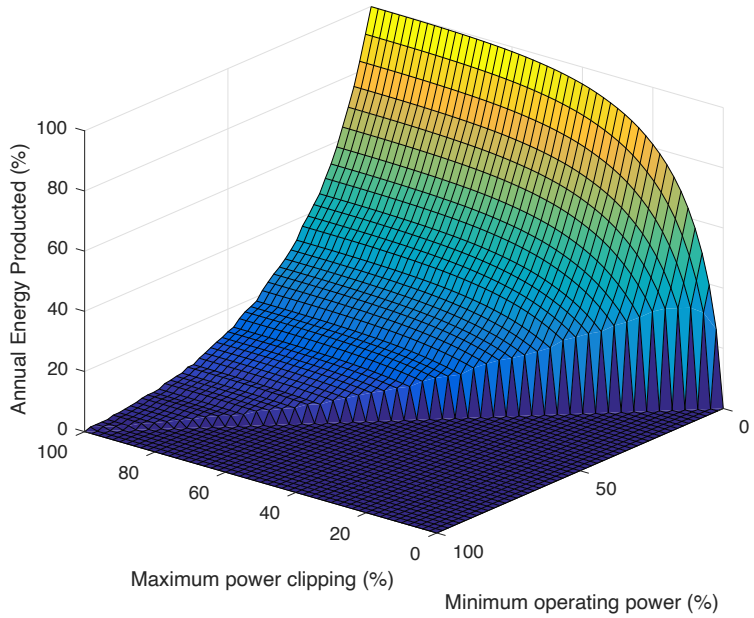

FIGURE 3.7: AEP rate of the bi-directional fixed axis direction tidal turbine.

The maximum of harnessed energy is around $15.21 MWh/m^2$. However, by choosing a cut-in speed of 1m/s the the harnessed energy decreases only by 2.47%. Figure 3.8 presents the AEP when the cut-in speed is equal to $1m/s$. Indeed, a power limitation around 30% of the maximal input power assure 90% of the total energy that can be harnessed.

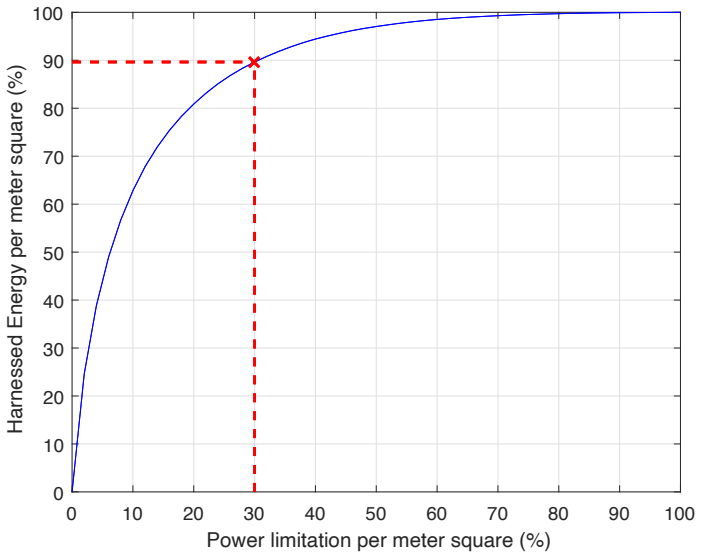

FIGURE 3.8: Harnessed energy rate versus power limitation rate.

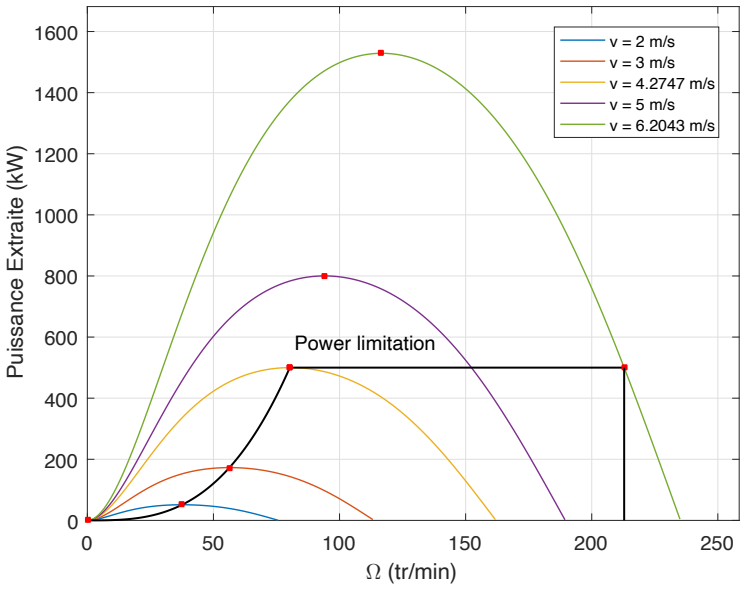

FIGURE 3.9: Power characteristic of a 500KW Tidal stream turbine.

The size of the tidal stream turbine depends on its power rating, therefore a limitation power around 30% of the maximum power is interesting in terms of energy production but also to avoid over-sized generators. When the input power exceeds the power rating, a power limitation strategy is adopted by accelerating the generator and therefore reducing the blades hydrodynamic efficiency (Power coefficient) [27]. Figure 3.9 illustrates the power characteristic of a 500KW tidal stream turbine.

Concerning the turbine rotor diameter (swept area), it is calculated by satisfying the condition that $P_r = 0.3P_{max}$.

3.2.4 Yaw drive-based tidal turbine

Even if a yaw system is adopted (figure 3.10), results shows relatively similar AEP compared to the fixed axis direction tidal turbine. Indeed, the AEP increases of 2.47% if the yaw system is employed. Moreover, a similar slight increase rate of 2.51% is calculated when the both systems have a cut-in speed equal to $1m/s$. Such results show that the Yaw system in the Ouessant site is not necessary. Furthermore, it can decrease the availability of the tidal turbine and AER accordingly.

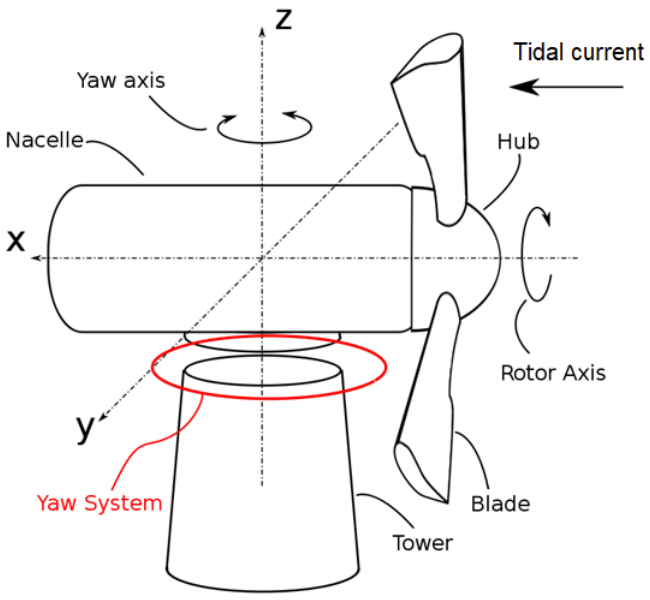

FIGURE 3.10: Schematic presentation of the yaw drive-based tidal turbine components.

3.3 Gearbox modeling

The gearbox is a system who converts the slow shaft rotational speed and high torque to a high rotational speed and low torque. It is generally characterized by: a rated input torque, a gear ratio, and a number of stages. The size and cost of the gearbox increases when one of the three previous parameters do. Concerning the gear train, it exists two main types: parallel shaft and planetary. In this thesis, two types of gearboxes are considered. The planetary single stage-gearbox and the two-stage gearbox which consists of a planetary gearbox connected to a parallel shaft one. The modeling in this subsection considers each stage apart.

3.3.1 Parallel shaft gearbox

The sizing of a single gear is based on the K-factor formula (eq. (3.8)) [93]. The k-factor indicates the tooth loads intensity, it can be calculated as the equation below. However, when the size of the gear is unknown it can be empirically estimated from [93].

$$K_f = \frac{W_t}{FWd}\frac{u+1}{u} \tag{3.8}$$

where $W_t = T_p\frac{2000}{d}$ is the tangential driving force, d is the gear diameter in millimeters, FW is the gear face width in millimeters, u is the gear ratio, and T_p is the torque applied to the gear.

Therefore, the size can be estimated by the following equation

$$FWd^2 = \frac{2000T_p}{K_f}\frac{u+1}{u} \tag{3.9}$$

The gear weight estimation is given by the following equation

$$G_{gear_e} = W_c\frac{K_{ag}FWd^2}{36050} \tag{3.10}$$

where W_c is the weight constant, K_{ag} is the application factor.

The application factor, sometimes know as the service factor, considers external factors that cause more load to the teeth then in perfect conditions. In fact, an application factor of 1.0 is chosen when we have a perfectly smooth turbine driving a perfectly smooth generator always at a constant speed (no frictions and no vibrations).

Accordingly, by considering the high load fluctuations due to the high marine energy density [94], an application factor of 1.25 is chosen.

In the case of a parallel shaft gearbox, the estimated weight is the sum of the two gears weight as the following equation shows

$$G_{gear_e} = W_c \frac{K_{ag}(FWd_1^2 + FWd_2^2)}{36050} \tag{3.11}$$

where d_1 and d_2 are the pitch diameter of the two parallel gears (fig. 3.11),

A parallel shaft gearbox has a gear ratio u proportional to the the ratio between the two gears diameters, where $u = \frac{d1}{d2}$. Therefore, the precedent equation becomes

$$G_{gear_e} = W_c \frac{K_{ag} FWd_2^2(u^2 + 1)}{36050} \tag{3.12}$$

Considering the equations (3.9) and (3.12), the total estimated weight of a parallel shaft gearbox is:

$$G_{gear_e} = W_c \frac{K_{ag}}{18.025} \frac{T_{p2}}{K_f}(u^2 + u + 1 + \frac{1}{u}) \tag{3.13}$$

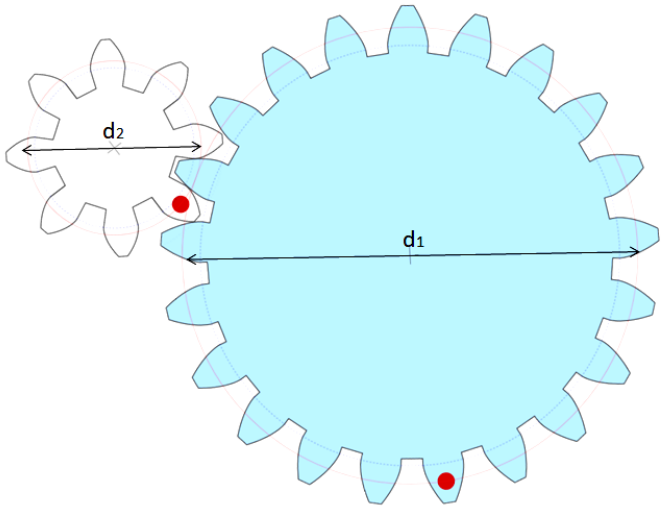

FIGURE 3.11: Illustration of a parallel shaft gear.

3.3.2 Planetary gearbox

The planetary gearbox has a high power density compared to parallel shaft one. However, its design is more complicated as shown in Figure 3.12. It consists of the sun, ring, , Z planet gears, and a carrier which is connected to all the planet gears

axles. The input shaft is connected to the carrier and the output one is connected to the sun gear. The gear ratio between the carrier and the sun gear is named u_s.

The sun gear volume is presented below

$$FWd_s^2 = \frac{2000T_s}{ZK_f}\frac{u_{sn}+1}{u_{sn}} \tag{3.14}$$

where d_s is the sun gear diameter, $u_{sn} = 0.5u_s - 1$ is the speed ratio between the sun and planet gears and T_s is the sun gear torque, which is considered as the output shaft torque.

The planet gear volume is:

$$FWd_p^2 = FWd_s^2u_{sn}^2 = \frac{2000T_s}{ZK_f}\frac{u_{sn}+1}{u_{sn}}u_{sn}^2 \tag{3.15}$$

Concerning the ring gear volume, it depends on its diameter and its thickness. Therefore, a scaling factor $K_r = 0.4$ is introduced and it is selected from [93], [95].

$$V_{rg} = K_rFWd_s^2(\frac{d_{rg}}{d_s})^2 = K_r\frac{2000T_s}{ZK_f}\frac{u_{sn}+1}{u_{sn}}(u_s-1)^2 \tag{3.16}$$

where d_{rg} is the ring diameter and $\frac{d_{rg}}{d_s} = u_s - 1$.

Knowing the volume of each part of the planetary gearbox and considering the equation (3.10), the planetary gearbox weight can be calculated as below:

$$G_{gear_p} = W_c\frac{T_sK_{ag}}{(18.025)K_f}\left[\frac{1}{Z} + \frac{1}{Zu_{sn}} + u_{sn} + u_{sn}^2 + \frac{K_r}{Z}(1+(u_{sn})^{-1})(u_s-1)^2\right] \tag{3.17}$$

3.3.3 Two-stage gearbox design

The two-stage gearbox configuration consists of a planetary gearbox connected to a parallel shaft gearbox. The output shaft of the planetary gearbox is connected to the input one of the parallel shaft one. Therefore, The gear ratio of two-stage gearbox is $u_2 = u_pu_e$, where u_p is the planetary gearbox ratio and u_e is the parallel shaft gearbox ratio. Concerning the optimal gear ratio combination for a specific u_2 gear ratio, only discrete gear ratios are considered and all possibilities are compared. The optimal gear ratio combination is the one equivalent to the lowest gearbox weight and cost.

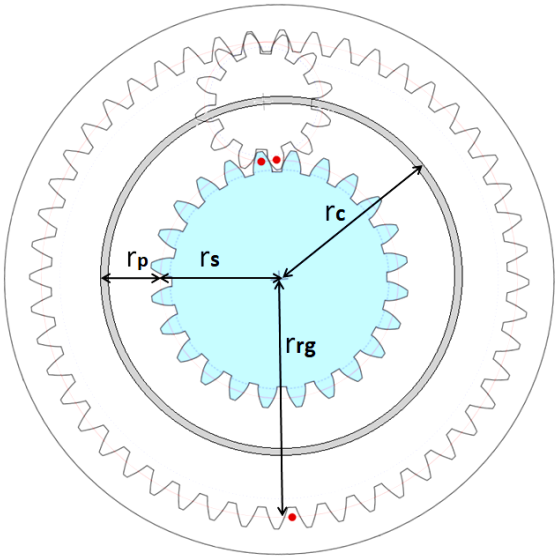

FIGURE 3.12: Illustration of a planetary gearbox with 1 planet gear. r_s is the sun gear radius, r_p is the planet gear radius, r_{rg} is the ring gear radius, and r_c is the carrier radius

3.3.4 Gearbox cost estimation

The cost estimation of a gearbox can be calculated basing on its total weight as the following equation presents

$$C_{gear} = c_{gear} G_{gear} \tag{3.18}$$

where G_{gear} is the gearbox weight and $c_{gear} = 6[€/kg]$ is the gearbox specific cost [55].

3.3.5 Gearbox losses

Concerning losses, they are difficult to estimate precisely. However, a simple approximation can be obtained by neglecting power dependent losses and considering only speed dependent ones [96].

$$p_{gear} = k_g P_N \frac{n_r}{n_{r_N}} \tag{3.19}$$

Equation (3.19) estimates gearbox losses for a single stage gearbox where k_g is the speed-dependent losses constant, P_N is the rated power of the TST, n_r is the rotational shaft speed, and n_{r_N} is the rated rotational shaft speed. In the case of a multiple-stage gearbox the power losses are added.

3.4 Permanent magnet generator design

A three phase radial flux permanent magnet generator is chosen for the three drive-train configurations: direct-drive, single-stage gearbox drivetrain, and the two-stage gearbox drivetrain. Indeed, such generator topology had the lead in the wind turbine industry as chapter 2 shows.

Figure 3.13 presents the geometric parameters and the structure of a one pair of poles. As the figure shows, the magnets are surface mounted and the generator curvature is assumed insignificant. For design purposes, the adopted modeling is a 2D analytical electromagnetic model based on magnetic circuit calculation [97], [12]. The objective is to calculate the generator size and cost according to its electromagnetic specifications.

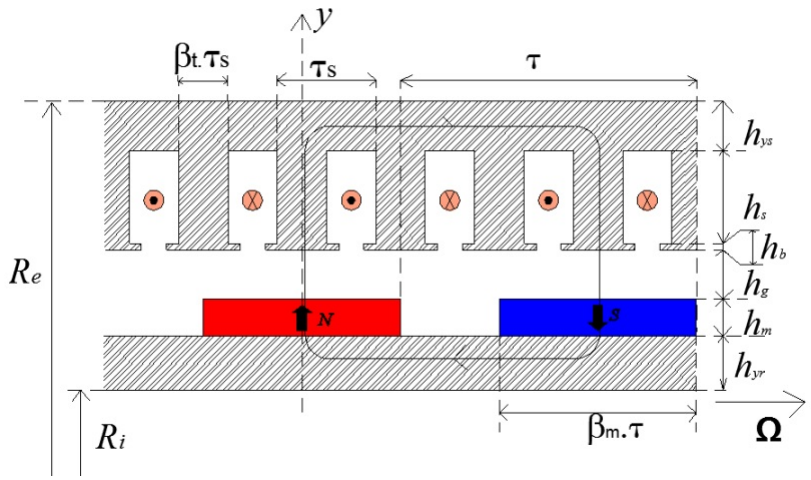

FIGURE 3.13: Basic dimensions of one pair of poles [27].

3.4.1 Electromagnetic torque

The average electromagnetic torque is a result from the interaction between the fundamental electromotive forces and the phase currents (considered sinusoidal) at the rated operating point [97]. This torque is assumed to be equal to the input mechanical torque.

$$< T_{EM} >= 4\sqrt{2} A_L k_{b1} B_{g_{max}} R_s^2 L_e \sin(\beta_m \frac{\pi}{2}) |\cos(\psi)| \tag{3.20}$$

where A_L is the current loading in the stator, $B_{g_{max}}$ is the maximum air-gap flux density under the magnet, k_{b1} is the first harmonic winding factor, ψ is the phase shift between the fundamental of the electromotive force and the current, R_s is the stator radius, L_e is the equivalent core length.

3.4.2 Air-gap

The following empirical formula presents the mechanical air-gap [98]

$$h_g = 2k_D R_s \tag{3.21}$$

Where the coefficient k_D considers the deformations caused by the forces acting on the rotating rotor.

The additional Carter air-gap $h_{g'}$ is calculated as [98]

$$h_{g'} = (k_c - 1)(h_g + \frac{h_m}{\mu_{rm}}) \tag{3.22}$$

Where k_c is the Carter factor, h_m is the magnet height, and $\mu_{rm} = 1$ is the magnets relative permeability.

The carter factor is given as below

$$\begin{cases} k_c &= \frac{1}{1+\sigma\frac{w_t}{\tau_s}} \\ \sigma &= \frac{2}{\pi}\left[tan^{-1}\left(\frac{w_t}{2h_m}\right) - \frac{h_m}{w_t} ln\left[1+\left(\frac{w_t}{2h_m}\right)^2\right]\right] \end{cases} \tag{3.23}$$

where w_t is the teeth opening width, τ_s is the slot pitch (fig. 3.14).

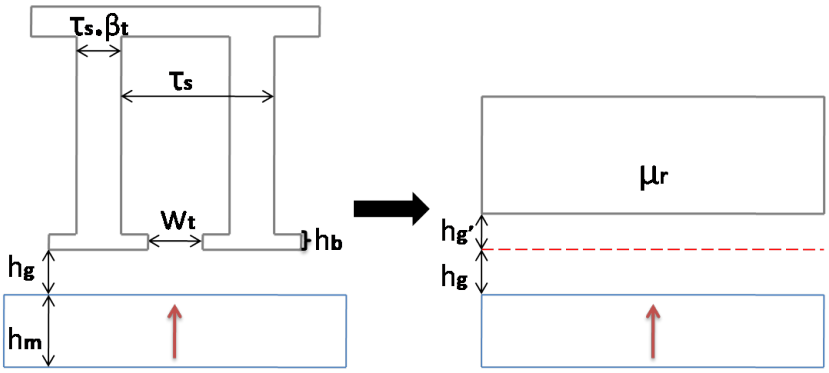

FIGURE 3.14: Additional carter air-gap concept

3.4.3 Magnet height

The magnet height model calculation considers inter-polar 2D leakage flow.

$$h_m = \frac{\tau_p}{2\pi}\left[\ln\left(\frac{B_{g_{max}} \exp\frac{-\pi}{\tau_p}(h_g + h_{g'}) - B_r}{B_{g_{max}} \exp\frac{\pi}{\tau_p}(h_g + h_{g'}) - B_r}\right)\right] \tag{3.24}$$

Where B_r is the magnets remanent flux density, $B_{g_{max}}$ is the maximum air-gap flux density, and τ_p is the pole pitch.

3.4.4 Slot height

The slot height is a function of the current loading A_L, the fill factor k_f, and the teeth pitch ratio β_t.

$$h_s = \frac{A_L}{k_f J(1-\beta_t)} \tag{3.25}$$

3.4.5 Stator and rotor yoke height

The stator yoke height h_{ys} is developed in a way to avoid saturation when the magnetic field is at its maximum. Concerning the rotor yoke, it is approximately equal to the stator one as approximately the same magnetic field traverse it.

$$h_{ys} = \beta_m \frac{\pi R_s}{2p} \frac{B_{g_{max}}}{B_{sat}} + \frac{1}{3} \frac{\mu_0 \sqrt{2} A_L \pi^2 R_s^2}{(h_m + h_g + h_{g'}) S_{pp} m p^2 B_{sat}} \tag{3.26}$$

$$h_{yr} \approx h_{ys} \tag{3.27}$$

where S_{pp} is the number of slots per pole per phase, m is the phases number, and p is pole pairs number.

3.4.6 Teeth pitch ratio

The teeth pitch ratio β_t is developed with the same principle as the stator yoke is developed. It is calculated to assure a non saturation of the generator when it is over-fluxed ($\psi = \pi/2$) and the air-gap flow density is at its maximum $Bg = Bg_{max}$ along the pole.

$$\beta_t = \frac{B_{g_{max}}}{B_{sat}} + \frac{\mu_0 \sqrt{2} A_L \pi R_s}{(h_m + h_g + h_{g'}) S_{pp} m p B_{sat}} \tag{3.28}$$

3.4.7 Maximum magnetic field

The maximum magnetic field H_{max} has to be less than the PM coercive magnetic field H_{cj} in order to avoid an irreversible permanent magnet demagnetization. The maximum magnetic field is developed considering the case where the rotor flow density and the stator flow density are opposite to each other. The maximum magnetic field is introduced in the next chapter as a constraint to the design optimization.

$$|H_{max}| = \frac{\sqrt{2}A_L \pi R_s}{(h_m + h_g + h_{g'})S_{pp}mp} + \frac{(h_g + h_{g'})B_{g_{max}}}{\mu_0 h_m} \tag{3.29}$$

Iron and copper losses

The specific iron losses are estimated by using the Steinmetz formula [99], [100]

$$p_{Fe} = 2p_{Fe0h}(\frac{f_e}{f_0})(\frac{\widehat{B}_{Fe}}{\widehat{B}_0})^2 + 2p_{Fe0e}(\frac{f_e}{f_0})^2(\frac{\widehat{B}_{Fe}}{\widehat{B}_0})^2 \tag{3.30}$$

Where $p_{Fe0h} = 2W/kg$ is the specific hysteresis loss, f_e is the field frequency in the iron, $p_{Fe0e} = 0.5W/kg$ is the specific eddy current loss in the laminated stator core for a frequency $f_0 = 50Hz$ and a flux density $\widehat{B_0} = 1.5T$. The total iron losses depends on the iron weight of the laminated stator as described below.

$$P_{Fe} = p_{Fe}G_{S_{iron}} \tag{3.31}$$

where $G_{S_{iron}}$ is the total iron weight of the stator.

Concerning copper losses, they are calculated as the following equation

$$P_{Cu} = \rho_{Cu}V_{S_{iron}} \tag{3.32}$$

where $\rho_{Cu} = 1.677910^{-8}\Omega.m$ is the electrical resistivity of the copper, $V_{S_{iron}}$ is the iron total volume of the stator.

accordingly, the electric yield is approximately calculated as below

$$\eta_{elec} = 1 - \frac{P_{Cu} + P_{Fe}}{< T_{EM} > \Omega} \tag{3.33}$$

where Ω is the rotational speed of the generator.

Electromotive force

The electromotive force first harmonic can be calculated as the following equation

$$E_1 = \frac{1}{\sqrt{2}}k_{b1}B_{g_{max}}R_s^2 L_e \Omega \tag{3.34}$$

When $\Omega[rad/s]$ is the rotational speed of the rotor, $B1$ is the amplitude of the first harmonic air gap flux density. $B1$ is calculated basing on a three level signal which equal to $+B_{gmax}$ above a north magnet, equal to $-B_{gmax}$ above a south magnet, and

equal to 0 between the two magnets. The air-gap flux density is assumed constant through a radial axis.

$$B_1 = \frac{4}{\pi} B_{gmax} sin\left(\beta_m \frac{\pi}{2}\right) \tag{3.35}$$

$\beta_m = 0.7$ is the magnet pitch ratio.

Synchronous inductance

The synchronous inductance L_s is the sum of the magnetizing inductance L_{sm} and the leakage inductance L_{sl}. the leakage inductance includes the end-winding leakage L_{end}, the slot leakage L_{slot}, and the skew leakage which is ignored as the generator is not skewed [98]. The synchronous inductance calculation is necessary to model the generator equivalent electric circuit, its power factor, and to evaluate its controllability. The inductance calculation considers a single layer stator winding with a diametral pitch and a slot number per pole per phase $S_{pp} = 1$.

The magnetizing inductance is calculated as below [98]

$$L_{sm} = \frac{2m\mu_0 R_s L_e (k_{b1} N_s)^2}{\pi p^2 (h_g + h_{g'})} \tag{3.36}$$

where N_s is the number of turns of the phase winding.

Regarding the slot leakage inductance, its estimation depends on the slot permeance coefficient λ_s for an open rectangular slot width w_s and height h_s [101]. The slot is assumed to be filled uniformly.

$$\lambda_s = \frac{1}{3} \frac{h_s}{w_s} \tag{3.37}$$

As the slot are semi-closed, an additional permeance coefficient λ_t is introduced

$$\lambda_t = \frac{h_b}{w_t} \tag{3.38}$$

The slot leakage inductance is therefore presented as below

$$L_{slot} = 2p\mu_0 L_e N_s^2 (\lambda_t + \lambda_s) = 2p\mu_0 L_e N_s^2 \left(\frac{1}{3}\frac{h_s}{w_s} + \frac{h_b}{w_t}\right) \tag{3.39}$$

The end-winding leakage inductance estimation is difficult to estimate. However a simple approximation based on the sum of the leakage inductance of each coil

without considering the mutual coupling between coils. The estimation is presented below [101, 102]

$$\begin{cases} L_{end} &= \frac{1}{2} p \mu_0 d N_s^2 ln \left(\frac{4d}{\xi} - 2 \right) \\ d &= \frac{\pi}{p} \left(R_s + \frac{h_s}{2} \right) \\ \xi &= 0.447 \sqrt{A_{slot} k_f} \end{cases} \tag{3.40}$$

where d is the end winding diameter, $A_{slot} = h_s(1 - \beta_t)\tau_s$ is the slot area, and k_f is the winding fill factor.

The phase synchronous inductance is therefore given as

$$L_s = L_{sm} + L_{sl} = L_{sm} + L_{end} + L_{slot} \tag{3.41}$$

Equivalent per-phase circuit

The equivalent per-phase circuit is illustrated in fig. 3.15. The stator phase resistance r_s is calculated basing on the coils size. The resistance consists of an end winding resistance and an active resistance.

$$r_s = \rho_{Cu} \frac{l_a + l_{ew}}{\frac{k_f A_{slot}}{N_s}} \tag{3.42}$$

where $l_a = L_e N_s 2p$ is the length of the active conductors per phase and $l_{ew} = 0.5\tau\pi N_s p$ presents the end winding conductor length. According to the equivalent

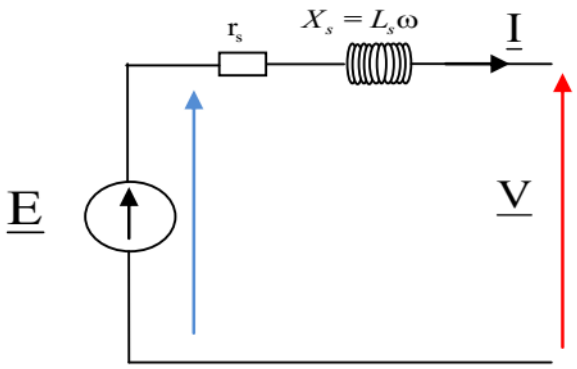

FIGURE 3.15

electrical circuit the phase voltage can be calculated as below:

$$V = \sqrt{(E - r_s I cos(\phi) - X_s I sin(\phi))^2 + (X_s I cos(\phi) - r_s I sin(\phi))^2} \tag{3.43}$$

Concerning the power factor FP, it is calculated when the torque is at its maximum which is equivalent to a phase of $\phi = \pi$.

$$FP(\Omega) = \frac{E(\Omega) - r_s I}{V(\Omega)} \tag{3.44}$$

3.4.8 Power electronic converter design

To inject power from the generator to the grid, a two level back-to-back Pulse Width Modulation (PWM) full scale converter is adopted. Its cost is estimated by using a specific power electronic cost $c_{conv} = 40€/kW$. Concerning losses rate, they are considered to be about 3% at the rated power. [103].

3.5 Conclusions

This chapter presents the modeling of the main tidal stream turbines components in addition to the marine current resources. In this context, the marine current resources are considered, where the AEP is modeled according to the power limitation and the cut-in marine current speed. Afterwards, the presence or not of a yaw system is discussed, where the results shows that a bi-directional fixed axis tidal turbine is more relevant. Accordingly, the optimal direction is calculated for an optimal harnessing of energy. than, the power limitation (the rated power) is discussed, where the results shows that a limitation on power of only 30% leads to a production of 90% of the total site energy. Considering the limitation rate, the rotor turbine diameter (blades) equivalent to a specific power rating can be calculated.

Secondly, an analytical design model of two gearbox types (planetary gearbox and parallel shaft gearbox) is proposed. Such model estimates the gearbox weight and cost which allows the cost estimation of even multiple-stage gearboxes. Moreover, losses calculation method of the single-stage gearbox and the two-stage one are presented.

The last part in this chapter focuses on the two-dimensional analytical design modeling of the permanent magnet generator. The main generator size parameters are considered in this part and expressed according to the physical parameters basing on Maxwell's equations. Furthermore, a rough estimation of the power electronic converters is presented.

4. Optimal design of a tidal stream turbine

4.1 Introduction

The objective of this chapter is to optimize the tidal stream turbine design by considering different drivetrain configurations (direct-drive, single-stage gearbox, two-stage gearbox). In this context, the design method is highlighted, than the cost function is presented and reformulated to be usable in the design process. Design constraints and assumptions are afterwards cited. Lastly, the designed tidal stream turbine with different drivetrain configurations and gearbox specifications are presented, compared, and discussed.

4.2 Design optimization method

The design optimization of an electrical generator is highly non-linear constrained multivariable problem. The cost function $C(X)$ is presented by the tidal stream turbine estimated cost. It is is the sum of all the tidal stream turbine subsystems cost as illustrated below

$$C(X) = C_g(X) + C_{gear} + C_{conv} \tag{4.1}$$

where $C_g(X)$ is the generator active material cost, C_{gear} is the gearbox cost, and C_{conv} is the converter cost. As it is shown in the previous equation, only the generator depends on the design variables X, while the gearbox cost and the converter cost can be calculated basing on the system specifications (previously presented in chapter 3). The design variables are presented by the vector $X = (A_L, J, B_{g_{max}}, p, R_s)$, where A_L is the stator current loading, J is the stator current density, B_{gmax} is the maximum air-gap flux density under the magnet, p is the pole pairs number, and R_s is the stator radius.

The interior-point optimization technique is used to find the optimal design while satisfying design constraints. $\mathbb{D}$ is the set of possible solutions where the design constraints are satisfied (Figure 4.2).

$$X^* = \underset{G \in \mathbb{D}}{argmin} ||C(X)|| \tag{4.2}$$

Figure 4.1 is a flowchart that describes the design optimization procedure.

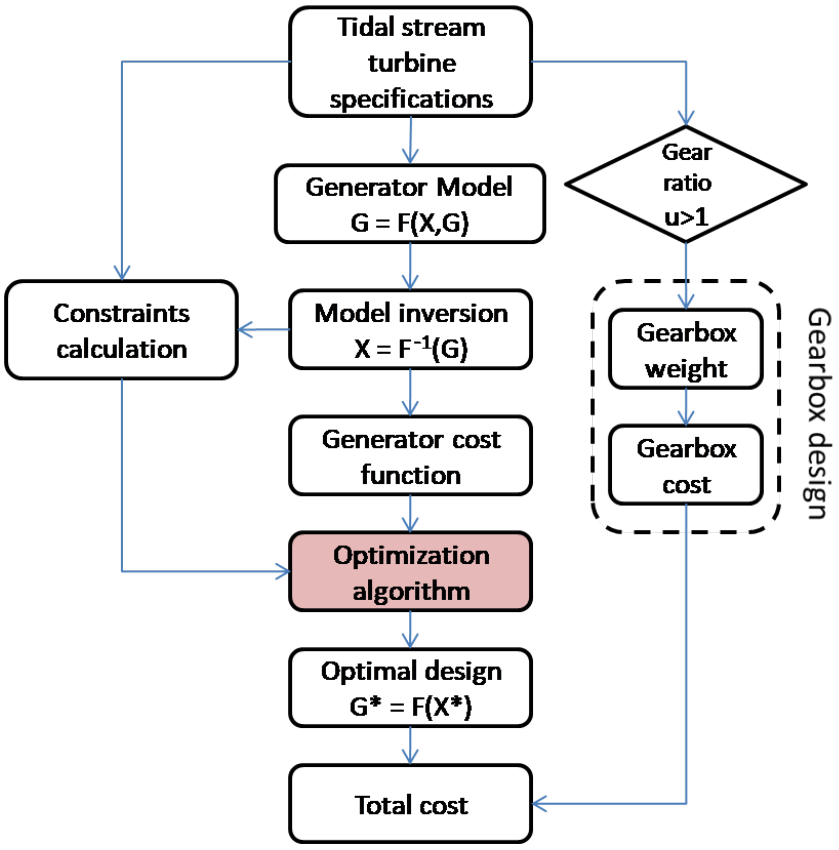

FIGURE 4.1: Flowchart describing the design optimization procedure.

4.2.1 Generator cost

The generator cost is estimated by calculating its active material cost, which depends on the weight/size of each material (copper, iron, electromagnet). Hence, the generator cost is calculated by its size parameters.

$$C_g = c_{Cu} G_{Cu} + c_{Fe} G_{Fe} + c_m G_m \tag{4.3}$$

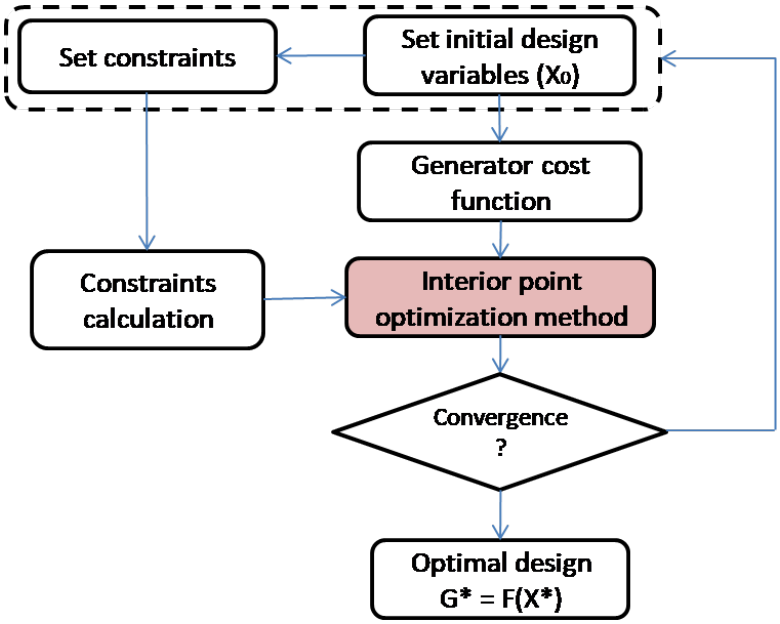

FIGURE 4.2: Flowchart describing the optimization algorithm.

where c_{Cu}, c_{Fe}, c_m are the copper, the iron, and the permanent magnet specific costs, and G_{Cu}, G_{Fe}, G_m are the copper, the iron, and the permanent magnet weights, respectively.

In this context, five size independent parameters are chosen by considering the generator model formulation in the previous chapter 3: the generator equivalent core length L_e, the slot height h_s, the magnet height h_m, the stator yoke height h_{ys}, and the teeth pitch ratio β_t. Those variable are gathered in one vector $G = (L_e, hs, hm, hys, \beta_t)$.

Generator model inversion

The generator model can be considered as a multi-input multi-output non-linear function $F(X, G) = G$ (equation (4.4)). Where the variable vector X presents the design parameters $X = (A_L, J, B_{g_{max}}, p, R_s)$. However, this formulation is not adapted to be used in the optimization cost function $C(X)$. Therefore a formulation of the generator model as $X = F^{-1}(G)$ is required to find the argument X_n of a given size vector G_n (Figure 4.3). In this specific context, two methods are adopted. The first one is based on an iterative inversion which is not heavy in terms of calculation time. The model equations are sorted according to their number of variables, where the first equation has the highest one.

$$G = F(X,G) \Longleftrightarrow \begin{cases} L_e &= \frac{<T_{EM}>}{\sqrt{2}A_L k_{b1} B_{gmax} R_s^2 \sin(\beta_m \frac{\pi}{2})|\cos(\psi)|} \\ h_s &= \frac{A_L}{k_f J(1-\beta_t)} \\ h_m &= \frac{\tau_p}{2\pi}\left[\ln\left(\frac{B_{gmax}\exp\frac{-\pi}{\tau_p}(h_g+h_{g'})-B_r}{B_{gmax}\exp\frac{\pi}{\tau_p}(h_g+h_{g'})-B_r}\right)\right] \\ h_{ys} &= \beta_m \frac{\pi R_s}{2p}\frac{B_{gmax}}{B_{sat}} + \frac{1}{3}\frac{\mu_0\sqrt{2}A_L\pi^2 R_s^2}{(h_m+h_g+h_{g'})S_{pp}mp^2 B_{sat}} \\ \beta_t &= \frac{B_{gmax}}{B_{sat}} + \frac{\mu_0\sqrt{2}A_L\pi R_s}{(h_m+h_g+h_{g'})S_{pp}mpB_{sat}} \end{cases} \tag{4.4}$$

The inversion process stops when two consecutive variable vectors X_k and X_{k+1} are less then a specific error $||X_k - X_{k-1}|| < \xi$ [104] (Figure 4.4). In the most cases the first method works, however when the inversion method doesn't converge, another inversion algorithm is adopted. The second method consists on minimizing the function $H(X) = ||F(X,G) - G||$ by employing a gradient based algorithm. The objective of this method is to find the root of the function H for a specific vector G. The result coincides with the argument of G (Figure 4.4).

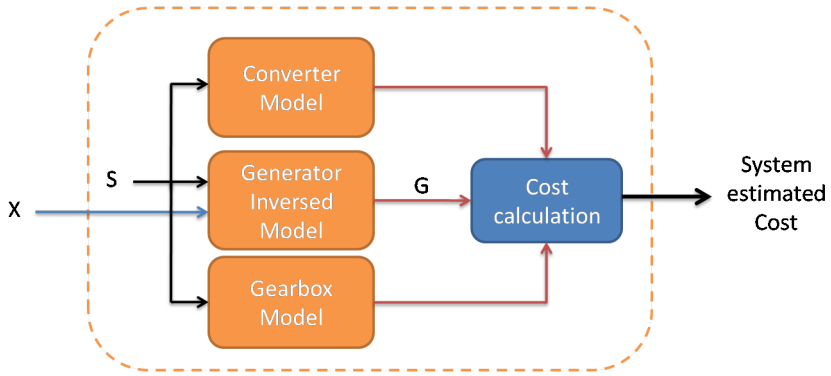

FIGURE 4.3: Illustration of the cost calculation model.

4.2.2 Optimization constraints

The optimization is performed under electromagnetic and mechanical constraints, which define the set $\mathbb{D}$ of possible solutions, where $X \in \mathbb{D}$.

4.2.3 Pole pair number

The first constraint, which concerns the pole pair number, is related to the maximum electrical frequency. In fact, a high pole pair number leads to a higher electrical

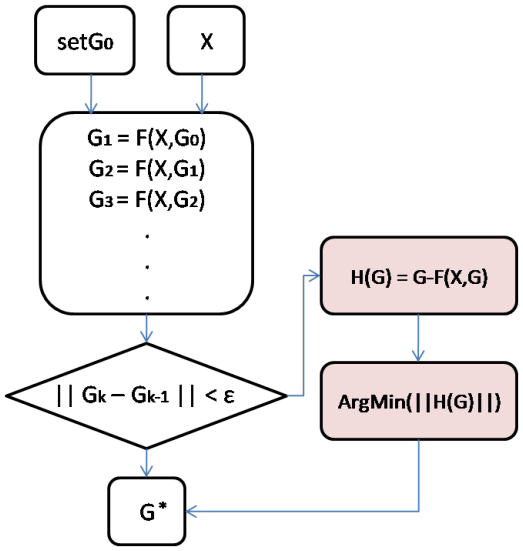

FIGURE 4.4: Illustration of the inversion algorithm.

frequency resulting in high iron losses. To avoid this, the maximum electrical frequency (f_{max}) allowed in laminated steel core is limited, which can be considered as a limitation of the pole pair number.

$$p_{max} = \frac{2\pi f_{max}}{\Omega} \tag{4.5}$$

4.2.4 Slot depth to slot width ratio

The second constraint is related to the ratio of slot depth h_s to slot width w_s. This ratio must be in the range of $4 - 10$ to avoid excessive mechanical vibrations, [105]. This limitation is expressed as the following inequality constraint

$$4 < \frac{h_s}{w_s} < 10 \tag{4.6}$$

4.2.5 Mechanical air-gap

The mechanical air-gap is 2 ‰the stator radius. However, a air-gap less than $h_{gmin} = 5mm$ is not allowed

$$h_g > h_{gmin} \tag{4.7}$$

4.2.6 Maximum magnetic field

To prevent demagnetization phenomena, the maximum magnetic field $H_{max}(X)$ (see equation (3.29)) should not be greater than the permanent magnet coercive field H_{cj}.

$$|H_{max}(X)| < |H_{cj}| \tag{4.8}$$

4.2.7 Current density and loading current

To avoid active cooling requirements, the current density J and the loading current A are limited in the range of $3 - 6\ A/mm^2$ and $40 - 60\ kA/m$ respectively [55].

$$J_{min} < J < J_{max} \tag{4.9}$$

$$A_{min} < A < A_{max} \tag{4.10}$$

Generator efficiency

The generator efficiency is considered to be greater than $\eta_{min} = 0.96$.

$$\eta_{elec}(X) > \eta_{min} \tag{4.11}$$

Phase voltage

The generator phase voltage root mean square is fixed to e equal to the converter voltage $V_{conv_m} = 690\ V$.

$$V(X) = V_{conv_m} \tag{4.12}$$

4.3 Design results and discussion

To investigate the cost-effectiveness of each drivetrain configuration, the design optimization of the three types of tidal stream turbine is performed. The obtained main design results for a power rating of 1.5MW are presented in the following table 4.1. The results consider a specific gear ratio selected beforehand for the two gearboxes: (3:1) gear ratio for the single stage gearbox and (9:1) gear ratio for the two-stage gearbox

TABLE 4.1: Optimal design parameters of the tidal stream turbine system.

Drivetrain configuration	D-drive	Multibrid (3:1)	2-stage GD (9:1)
Generator ($1.5MW$)			
Generator rated speed [rpm]	47.0	141	423
Generator rated torque [kN.m]	304.48	101.5	33.83
Air gap radius R_s [m]	1.604	1.001	0.665
Equivalent core length L_e [m]	6	10.3	18.8
Stator tooth pitch ratio β_t	0.55	0.53	0.42
Stator slot height h_s [mm]	47	46	46
Stator yoke height h_{ys}[mm]	12.1	12.2	12.2
Magnet height h_m [mm]	6.8	7.0	6.2
Generator efficiency η	0.97	0.98	0.98
Power Factor p_f	0.89	0.90	0.93
system weight [Ton]			
Iron	6.31	2.07	1.78
Copper	1.59	6.6410^{-1}	3.9710^{-1}
Permanent magnet	17.110^{-2}	5.9910^{-2}	2.4710^{-2}
Gearbox	0	0.67	7.47
Components cost [k €]			
Generator	24.04	8.82	4.58
Gearbox	0	4.02	44.82
Converter	60	60	60
Total Cost	84,04	72.84	109.4
Cost per energy [€/MWh]	73.5	63.70	95.70

As Table 4.1 shows, The direct-drive generator are heavier and larger than the two geared configurations. However, in terms of cost per energy, it is more advantageous than the two-stage gearbox driven generator. The two-stage gearbox have the cheapest generator with good performances. However, that advantage is paid by a heavy and expensive gearbox. Besides that, the Multibrid tidal stream turbine with a single-stage gearbox gather the advantages of the two other configurations. The generator is less expensive and lighter than the direct-drive one and its single-stage gearbox is smaller and cheaper.

4.3.1 Two-stage gearbox driven generator

The previous results consider only one gear ratio for the gearbox. In this part, the following gear ratios are considered: (9:1), (12:1), (15:1), (16:1), (20:1), (24,1). The first stage (connected to the input main shaft) is always a planetary gearbox and the second one is a parallel shaft one (connected to the generator). the chosen combinations are : (3:1)x(3:1), (3:1)x(4:1), (3:1)x(5:1), (4:1)x(4:1), (4:1)x(5:1), (4:1)x(6:1). The generator cost and gearbox cost are investigated in this part according

to the gearbox ratio variation (fig. 4.5). As the converter cost depends only on the power, it is not considered in the comparison.

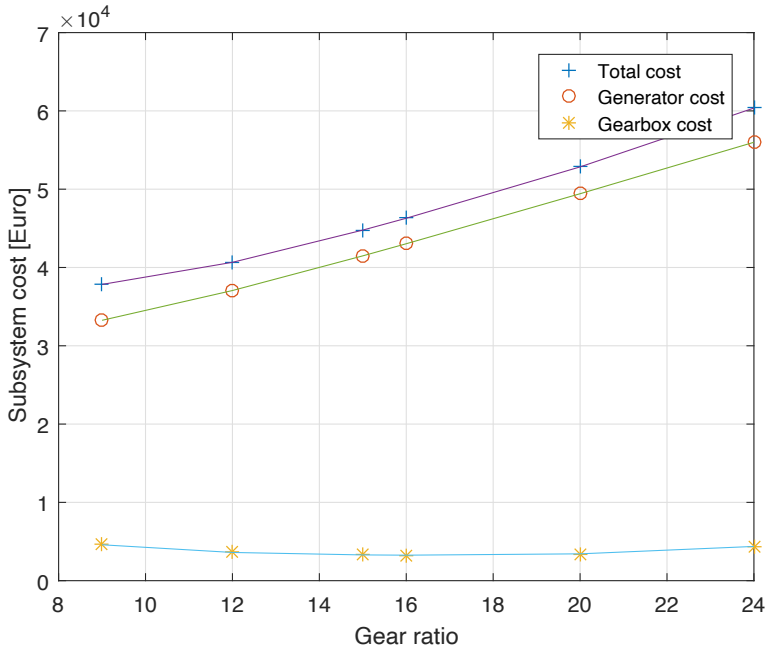

FIGURE 4.5: two-stage gearbox and generator cost (1.5 MW)

Figure 4.5 shows that the cost increases when the gearbox ratio does. Concerning the generator, its cost decreases slightly and after that increases when the gear ratio is (24:1). As the figure shows, the gearbox cost is much higher than the generator one. Therefore, the challenge with two-stage gearbox driven generators is more in the design of the gearbox than it is with the generator when a well designed gearbox can make a big difference.

Concerning the generators, the active materials cost variation according to the gear ratio are presented in Figure 4.6. The figure shows that copper cost is relatively similar with a slight decrease from (9:1) to (20:1). However, magnet cost decreases for high gear ratios. Iron cost increases with the gear ratio (20:1) and (24:1), which results in a slight increase in the relative generator total cost.

4.3.2 Single-stage gearbox driven generator (Multibrid)

As the previous subsection, this part focuses on the Multibrid generator with a single stage gearbox. The cost of the generator and gearbox are both investigated when the gearbox ratio varies. The considered gearbox ratios are : (3,1), (5,1), (7,1), (9,1), (11,1). In addition, the direct-drive configuration is also added with an equivalent gear ratio of (1:1) (fig. 4.7).

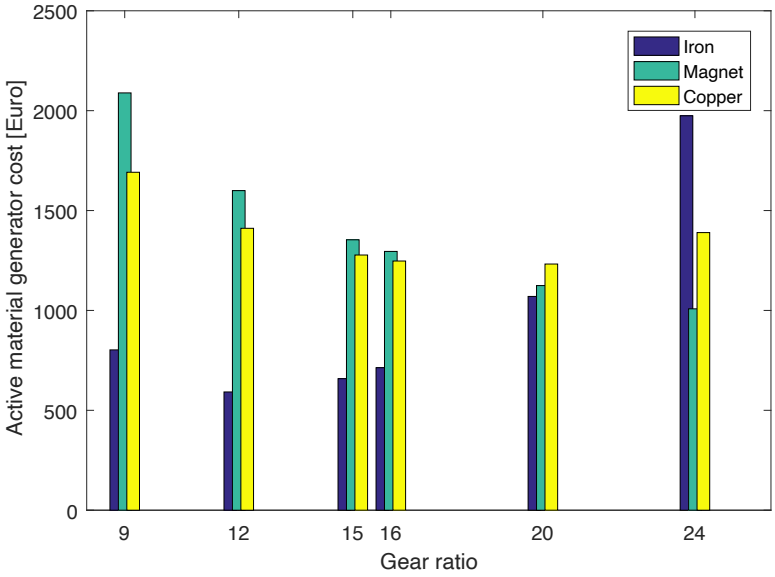

FIGURE 4.6: Active material cost of the two-stage gearbox driven generator (1.5 MW)

According to the optimal design results, adopting a planetary gearbox with a gear ratio of (3:1) results in a decrease of around 62% compared to the direct-drive generator cost which is a great advantage for Multibrid systems. However, for high gear ratios, the gearbox cost increases much higher than the decrease of the generator cost. Indeed, a system with a gear ratio of (9:1) is more expensive to the direct drive one. Moreover, a gear ratio around (3:1) and (5:1) seems promising even if the study does not consider the generator structure cost and the manufacturing cost. In fact, these two parameters gives an advantage to the Multibrid systems, which are compact, compared to the other drivetrain concepts.

The second part focuses only on the generator and presents its active material cost according to the gear ratio variations (fig. 4.8). It is obvious that the direct-drive generator have the highest cost. The magnet cost is the highest one among all the generators and it decreases with the decrease of the generator cost. The copper cost comes in the second place and the iron cost comes in the third one.

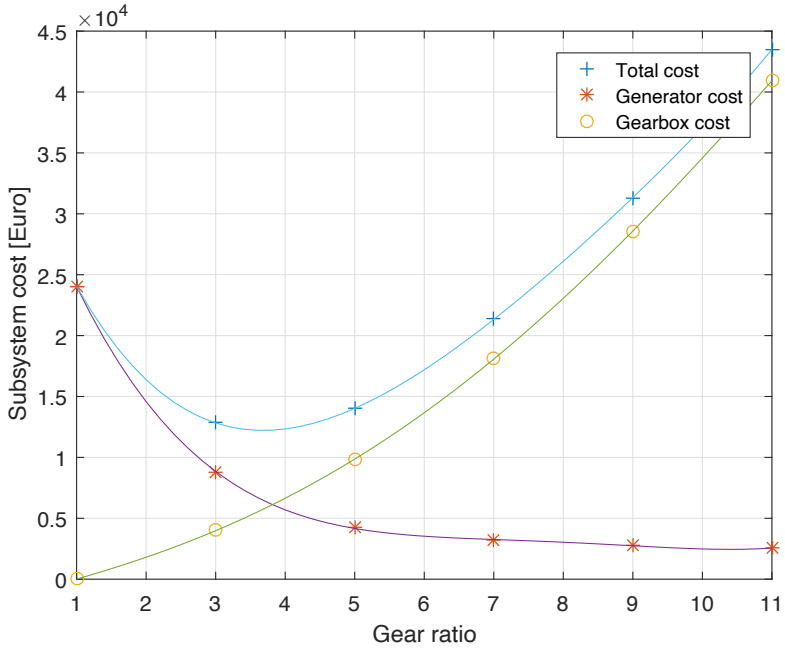

FIGURE 4.7: single-stage gearbox and generator cost (1.5 MW)

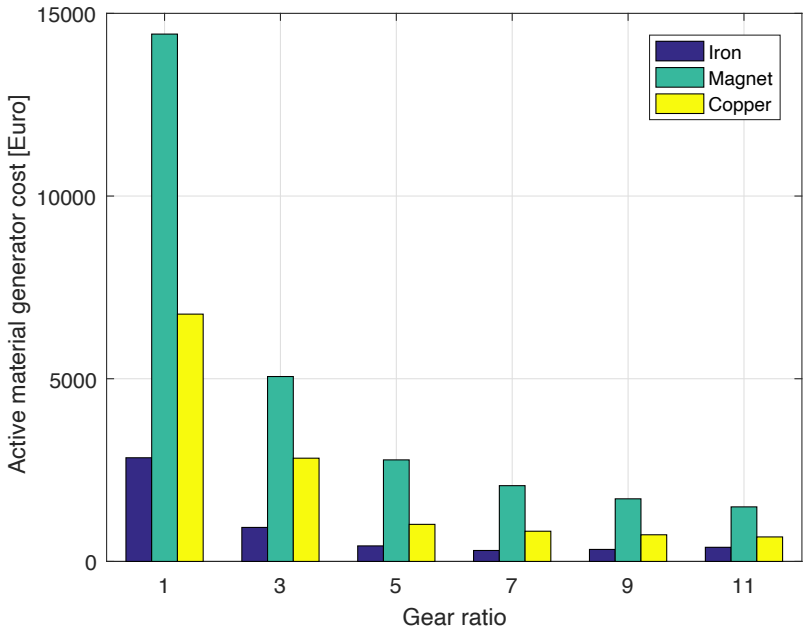

FIGURE 4.8: Active material cost of the Multibrid generator cost (1.5 MW)

4.3.3 Comparison: direct-drive, Multibrid, tow-stage gear drive

Figure 4.9 gives an overview on the gearbox and generator cost of the three configuration by considering multiple gear ratios. The results shows that the direct-drive cost

is lower than the cost of two-stage gearbox driven systems even if their generators are much cheaper. Concerning the multibrid configuration, it is advantageous for low gear ratios, however for high gear ratios its gearbox cost increases with a high rate contrary to the two-stage gearbox. The (3:1) single-stage gearbox driven generator is always the optimal one in terms of cost. Concerning the two-stage gearbox it seems advantageous compared to the Multibrid system when the gear ratio is high than (9:1), however its gearbox cost is much higher and accordingly the whole system is.

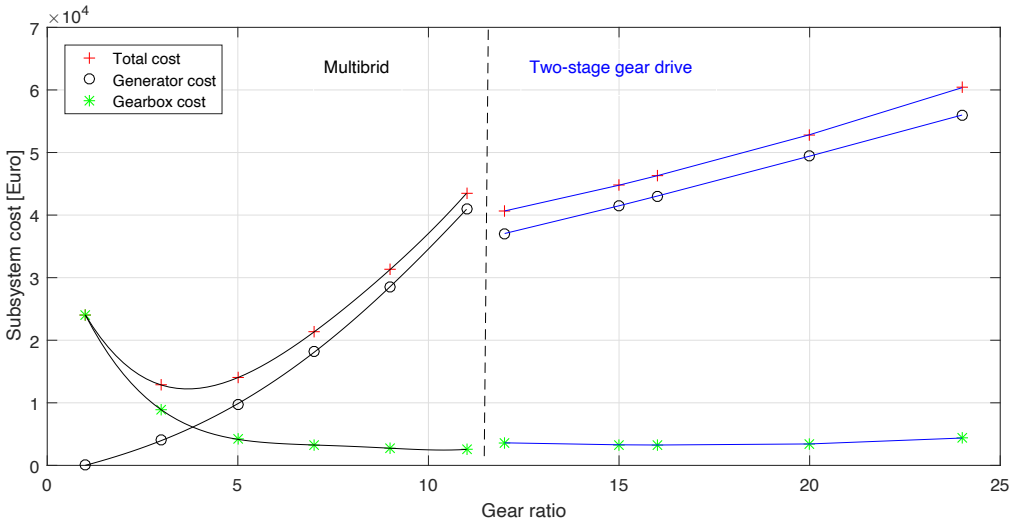

FIGURE 4.9: Generator and gearbox cost for three drivetrain configuration (1.5 MW)

Figure 4.10 shows the advantage of the two-stage gearbox when high gear ratios are adopted, which makes the single-stage planetary gearbox interesting only for low gear ratios (lower than (11:1)). The figure shows also how the concatenation of two gearboxes is preferable when high gear ratios are required.

4.3.4 Power rating variation: Multbird Vs. Direct-drive

The Multibrid concept in addition to the direct-drive one seems more suitable to tidal stream turbine applications according to the previous obtained results. Therefore, the two configurations are considered in the next subsections. To investigate the cost-effectiveness of the two configurations, not only the gear ratio is varied but also the power rating. In this case, the total harnessed energy differs and the cost per produced energy can be compared. The preferable power rating is also discussed by considering the Ouessant site energy potential. Three power ratings are adopted: 0.5 MW, 1.5 MW, and 5 MW. Figure 4.11 presents the estimated gearbox and generator

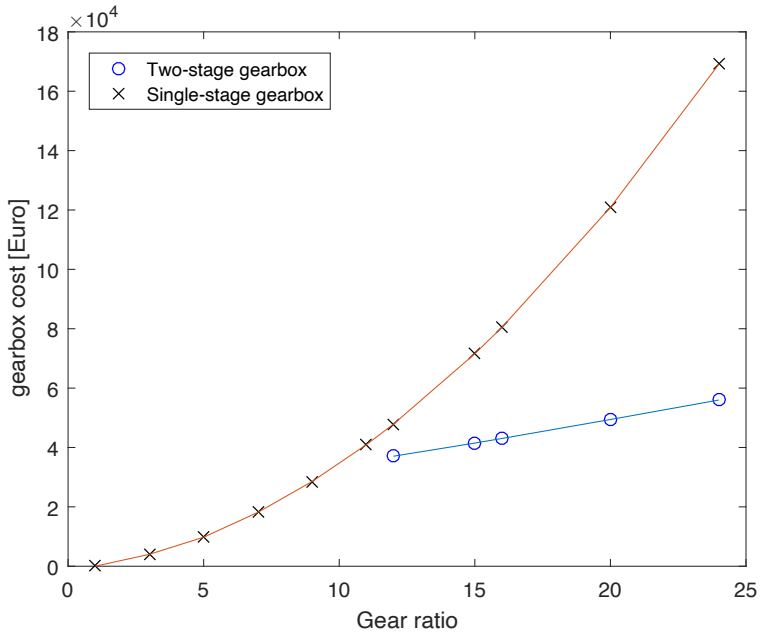

FIGURE 4.10: Generator and gearbox cost for three drivetrain configuration (1.5 MW)

cost for the three power ratings and for different gear ratios including the direct-drive configuration. The (3:1) single-stage gearbox driven system remains the optimal one for the three power ratings. Besides that, the cost increases when the gearbox ratio is more than (3:1), however the gap between the different power ratings systems cost for a specific gear ratio becomes greater when the gear ratio increases.

Otherwise, Figure 4.12 presents the total cost per MWh of the three power ratings. Indeed, The produced energy is estimated for each tidal stream turbine and taken as a reference. The obtained results shows that the direct-drive configuration cost per MWh is less sensitive to the power rating variation. Whereas, the Multirid configuration cost per MWh sensitivity increases with the increase of its gear ratio. Regarding the power rating choice, the $500kW$ seems advantageous especially if the considered system have a high gearbox ratio. Moreover, the $1.5MWh$ power rating is advantageous for gear ratios lower than (7:1). Concerning the $5MWh$ power rating systems, the estimations show that the cost per MWh is competitive in the case of low gear ratios, however the cost is not interesting for high gear ratios. In addition, a high power rating needs larger rotor turbines (blades). Indeed, a $5MW$ rated power requires a turbine rotor diameter of $18.8m$ which should be considered as a constraint according to the site deepness.

Table 4.2 presents the main parameters used to calculate the annual energy produced and the cost of each component.

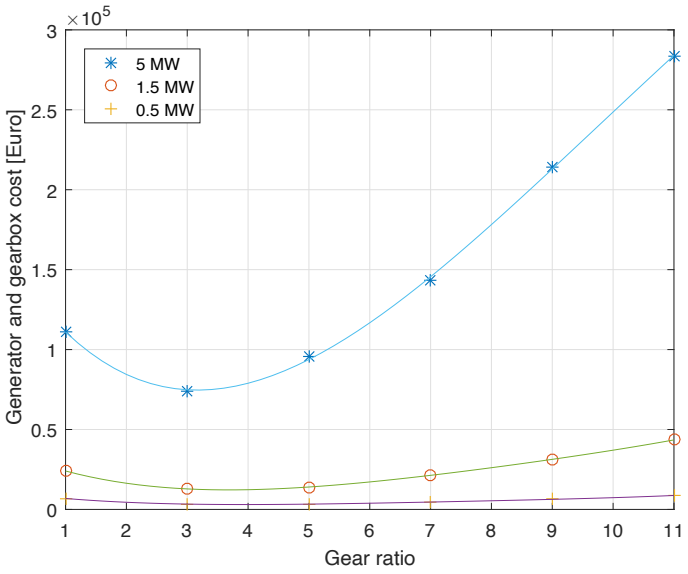

FIGURE 4.11: Generator and gearbox estimated cost.

TABLE 4.2: Modeling parameters of the tidal stream turbine system.

Tidal stream turbine			
Rated power P_N [MW]	0.5	1.5	5
Rated rotor speed n_{r_N} [rpm]	80.3	47.0	25.8
Rotor diameter D [m]	6	10.3	18.8
Cut it tidal current speed v_i [m/s]		1.0	
Cut out tidal current speed v_c [m/s]		6.2	
Maximum power coefficient C_{pmax}		0.455	
Optimum tip speed ratio λ_{opt}		5.90	
Sea water density ρ $[kg/m^3]$		995.6	
Single stage planetary gearbox			
Gearbox application factor K_{ag}			1.25
K-factor K_f $[N/mm^2]$			2.76
Gearbox weight constant W_c			0.3
Planet gears number Z			6
Gearbox specific cost c_{gear} [€/kg]			6
PMG system			
Specific cost of electrical steel c_{Fe} [€/mT]			449.77
Specific cost of copper c_{Cu} [€/mT]			4259.18
Specific cost of NdFeB magnet c_m [€/mT]			84538.60
Specific cost of power electronics c_{conv} [€/kW]			40

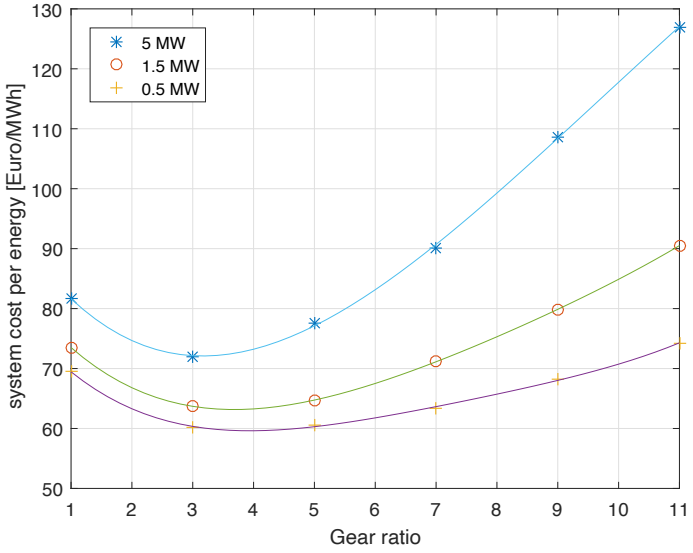

FIGURE 4.12: TST total estimated cost per MWh.

4.3.5 Optimal drivetrain configuration

The previous obtained results shows that the (3:1) single-stage gearbox driven tidal stream turbine is the optimal topology even if it differs slightly with the (5:1) single-stage geared one. It is also shown how the Multibrid concept in general presents a promising hybrid solution for tidal stream turbine applications. Such configuration can be an alternative to direct-drive one.

Figure 4.13 presents four poles of the designed (3:1) geared generator and Figure 4.14 shows a front and lateral view of the same designed generator at the rating power of $1.5MW$. The two figures give a vision of the designed generator structure and size.

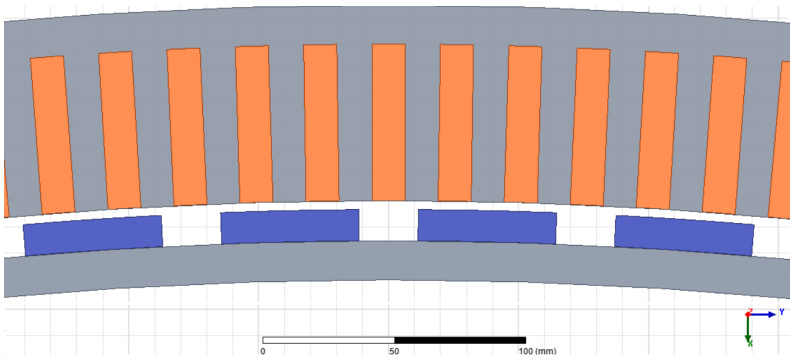

FIGURE 4.13: View of the designed (3:1) geared generator at the power rating of 1.5 MW.

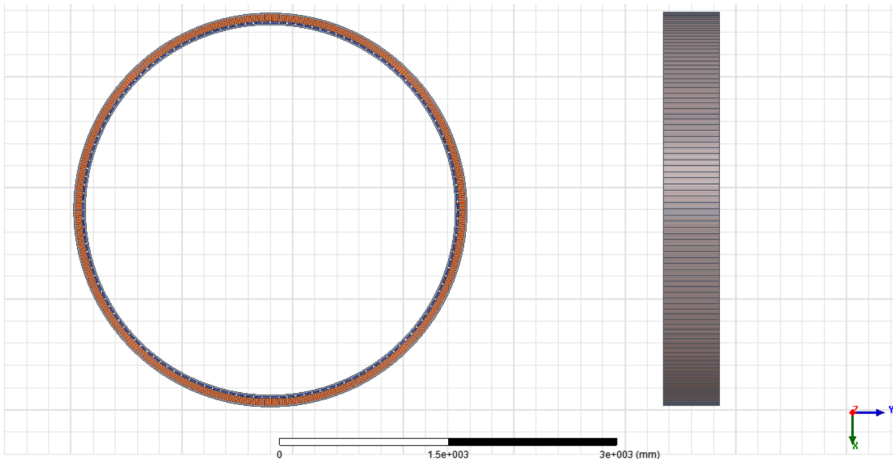

FIGURE 4.14: Front and lateral view of the designed (3:1) geared generator at the power rating of 1.5 MW.

The results can be slightly changed if more accurate cost estimations are adopted by considering other factors as: the generator structure and manufacturing costs and the foundations cost. Furthermore, a more accurate gearbox design can also affect the estimation results. However, the Multibrid concept potential as an alternative to usual designs remains. this comparative study results could be useful for TST designers and could give them a sight on the Multibrid concept relevance.

4.4 Conclusions

In this chapter, an investigation on the cost-effectiveness of different drivetrain configuration is performed. Firstly the design optimization process is described, where the analytical models presented in the previous chapter are reformulated to be properly used. Secondly, the optimal design results of typical drivetrain configurations, which are the direct-dive configuration, the Multibrid one, and the two-stage geared one, are presented for a power rating of $1.5MW$. The last part concerns a comparison between the three drivetrain configuration according to the gear ratio variations, where the optimal gear ratio is investigated. The comparison considers the gearbox cost, the generator cost, the total cost, and the cost per produced energy. The main conclusions are the following:

- The optimization results clearly shows that the Multibrid concept is a promising one for tidal stream turbine applications when compared to direct-drive or two-stage geared configuration.

- Among Multibrid systems, the ones with low gear ratios seems preferable, where the (3:1) gear ratio is the optimal one.
- The costs per produced energy rises with the increase of the gear ratio. The generator is one of the most costly components in direct-drive tidal stream turbines, which means that further developments on such components make the direct-drive concept more competitive. The two-stage gearbox design improvements present a challenge to allow tidal stream turbines with such gearbox more attractive.
- The cost per produced energy of $500kW$ and $1.5MW$ tidal stream turbines seems more advantageous if compared to the cost of $5MW$ ones especially for high gear ratios.
- The cost per produced energy of the direct-drive configuration is less sensitive to power rating changes compared to geared ones.

5. Design optimization of a magnetically-geared tidal turbine generator

5.1 Introduction

The objective of this chapter is to propose a design of a magnetically-geared tidal stream turbine. Firstly, the chosen magnetically-geared machine topology is introduced, where its operating principles are presented. Afterwards, the design methodology is highlighted, where a design optimization, based on finite element method, is performed for a $500kW$ pseudo-direct drive generator. The optimization focuses on maximizing the torque density under certain constraints as matching between the magnetic gearbox with the generator stator. The magnetically-geared generator design results are discussed and compared to the other drivetrain concepts: direct-drive one and mechanical geared ones.

5.2 Overview on the pseudo-direct drive generator

magnetically-geared generators (MGGs) are permanent magnet generators integrated with a magnetic gearbox which results in a compact machine. Many types of MGG exist and they differ according to the magnetic gearbox type and stator topology (see chapter 2). This chapter is devoted to the outer-stator magnetically-geared generator, where its gearbox is a flux modulated magnetic gear. such topology is also known by Pseudo-Direct Drive (PDD) ones [77] (figs. 5.1 and 5.2).

5.2.1 Pseudo-direct drive components

The pseudo-direct drive generator consists of:

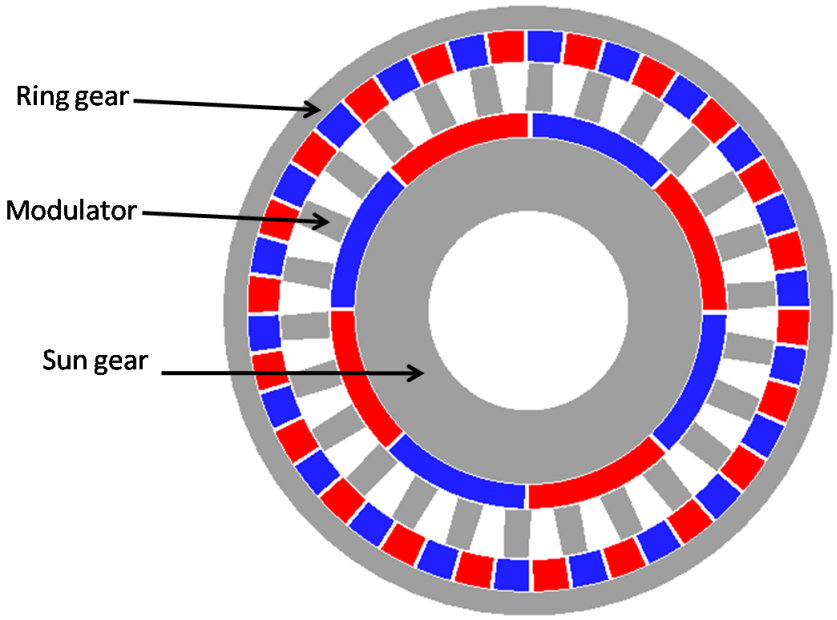

FIGURE 5.1: Layout of a flux modulated magnetic gearbox.

- A laminated outer stator with copper windings, where its inner bore is integrated with a stationary permanent magnet rotor called the ring gear (outer rotor of the magnetic gear).
- A sun gear (inner permanent magnet rotor) which is the high speed rotor.
- A modulator rotor which consists of ferromagnetic slots and rotates at a low speed and it is connected to the low speed shaft. the modulator assures the coupling between the sun gear and the ring gear.

Flux-modulated magnetic gear operating principles

Flux-modulated magnetic gearing is based on the ferromagnetic pole-pieces (modulator) which modulates the magnetic field created by the inner and the outer permanent magnet gears. Indeed, without a modulator there will be no coupling between the two rotors since the number of their poles is different. The coupling between the two rotors is maximized when the ferromagnetic pole pieces q_m presents the sum of the outer rotor pole pairs number p_r and the inner rotor ones p_s.

$$q_m = p_s + p_r \tag{5.1}$$

The torque on each rotor depends on the load angle δ_g, which can be expressed as below [106]

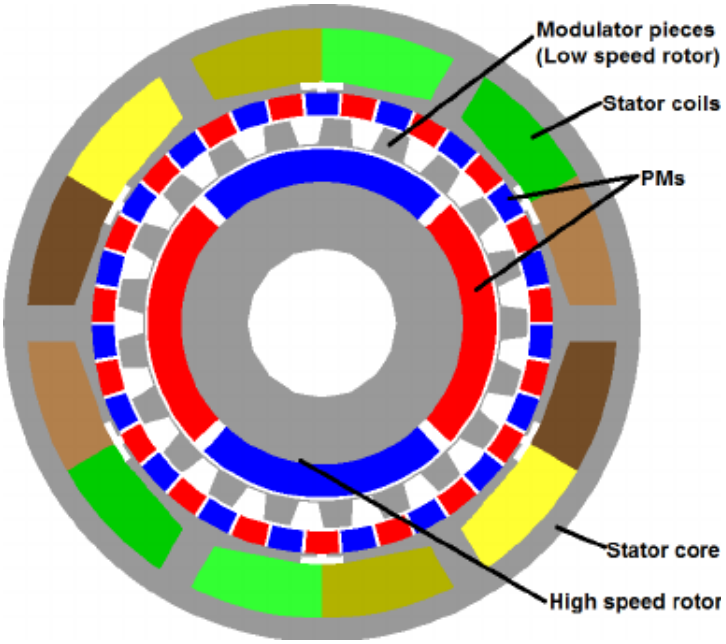

FIGURE 5.2: Layout of an outer-stator magnetically-geared generator.

$$\delta_g = p_s\theta_s + p_r\theta_r - q_m\theta_m \tag{5.2}$$

where θ_s, θ_r, and θ_m presents the angular position of inner rotor, the outer rotor, and the modulator respectively. Hence, the torque on the modulator can be presented as

$$T_m = T_{m_0} sin(\delta_g) \tag{5.3}$$

where T_{m_0} presents the stall torque which can be considered as the maximum transferable torque. In the case of an overload, the modulator will slip. For an operating point equivalent to a specific load angle δ_g, the derivative of equitation (5.2) leads to the following expression.

$$p_s\omega_s + p_r\omega_r - q_m\omega_m = 0 \tag{5.4}$$

5.2.2 Gear ratio

In the case of a pseudo-direct drive generator, the outer rotor is stationary and integrated with the stator $\omega_r = 0$. The gear ratio is therefore presented by the ratio between the high speed rotor and low speed one (modulator).

$$u_g = \frac{\omega_s}{\omega_r} = \frac{q_m}{p_s} = 1 + \frac{p_r}{p_s} \tag{5.5}$$

Concerning the torque transmission, the input torque is transmitted to both the sun gear T_s and the stator T_i (eq. (5.6)).

$$T_m = -u_g(T_s + T_i) \tag{5.6}$$

5.2.3 Adaptation between the generator and the gearbox

The design of a MGG have to consider both the stator and the magnetic gearbox in a way to avoid an over-sizing of one of them. Furthermore, if the stator rated torque is equivalent to the modulator stall torque, the magnetic gears will be vulnerable to splitting. In this case, a slight increase in the input torque lead to instability in the gearbox. Hence, a safety margin should be taken to avoid such phenomenon. In the other hand, if the rated torque is too low comparing to the modulator stall torque, a great part of energy will be transmitted to the sun gear. In this case, the MGG works as a torque divider which is not the objective. For this reason, a split ratio γ_i is introduced to illustrate the rate of transmitted torque [107, 108].

$$\gamma_s = u_g \frac{|T_{i_r}|}{|T_{m_r}|} = 1 - u_g \frac{|T_{s_r}|}{|T_{m_r}|} \tag{5.7}$$

T_{i_r} , T_{s_r} and T_{m_r} are respectively the rated stator torque, the sun gear stall torque, and the modulator stall torque. Their calculation is done from a single point finite element simulation under rated operating conditions. A split ratio greater than 0.8 is usually preferable.

5.3 Design optimization methodology

The design of the PDD generator is based on the finite element modeling using FEMM as a software of simulation. Concerning the optimization process, a gradient-based algorithm (Feasible direction method) is adopted. Basing on the finite element modeling, the torque density, as a cost function, is evaluated for an initial size G_0. Afterwards, the algorithm approximates the cost function by a first-order function to choose another size G_1 which have a higher torque density and so on. the process is repeated until an optimal design is found.

$$G^* = \underset{G \in \mathbb{D}}{max}(\tau_v(G)) \tag{5.8}$$

The design methodology is described by Figure 5.3.

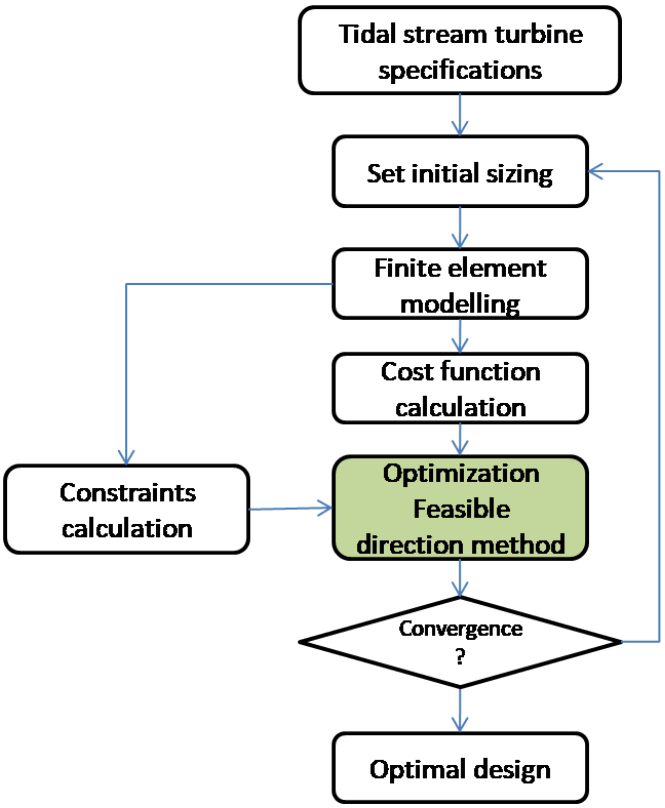

FIGURE 5.3: Layout of an outer-stator magnetically-geared generator.

The main pseudo-direct drive generator design parameters are presented by Figure 5.4.

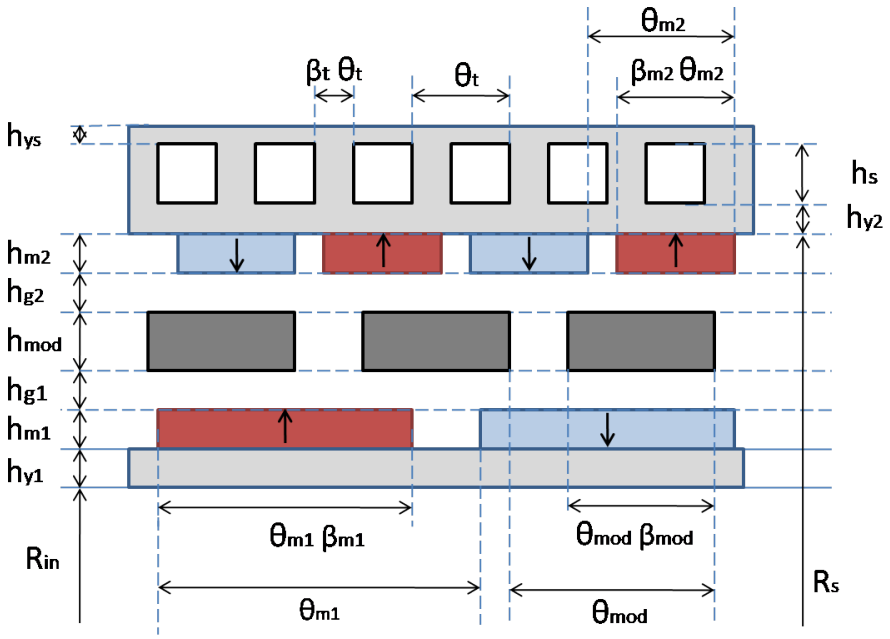

FIGURE 5.4: Basic dimensions of a one pole pair.

5.3.1 Fixed design parameters

In addition to the following fixed parameters, the design considers the tidal stream turbine specifications that have been previously used in Chapter 4.

Power rating

Even if the MGGs are still in their infancy, where usually low power prototypes are studied, a high power rating is considered in this study. Indeed, the objective is to propose a design procedure of such generator, optimize it, and afterwards estimates its cost to be compared to other generator types. As previously mentioned, the designed MGG have a power rating of $500kW$.

Pole pairs and stator tooth number

Pole pairs number of each rotor, in addition to the stator tooth number, are chosen before the design process. Such parameters affect the operating frequency, the cogging torque, the stall torque, and the gear ratio. Indeed, a cogging factor, which indicate the cogging torque amplitude, was presented in [109].

$$\tau_{cog} = \frac{2p_s q_m}{LCM(2p_s, q_m)} \tag{5.9}$$

where LCM is the low common multiple. Moreovere, according to [110, 111] fractional gear ratios seems preferable to reduce the cogging torque. In this context, the sun gear pole pairs number is chosen equal to $p_s = 4$, the ring gear ones are equal to $p_r = 31$, accordingly the pole pieces $q_m = 35$, and the gear ratio is $u_g = 8.75$. Concerning the tooth number, it is accordingly $Nt = 6p_s = 24$ as the winding is an overlap one.

Operating electrical frequency

the operating electrical frequency is calculated as below

$$f_0 = \frac{q_m \omega_m}{2\pi} = \frac{q_m n_{r_n}}{60} \tag{5.10}$$

where $n_{r_n}[rpm]$ is the rated input shaft rotor speed (table 4.1).

Mechanical air-gap

Mechanical air-gaps are not considered during the design process. They are assumed to be equal and For high stator diameters they presents 1 ‰of the diameter. However, when the air-gap is below $5mm$, it is instead fixed at this value.

5.3.2 Initial sizing

A initial sizing of the MGG is performed for a power rating of $500kW$ under rated operating conditions. In this context, other parameters are chosen or roughly estimated only for this purpose.

Stator sizing

The PDD generator size is roughly estimated to be used as an initial design. In this context, some assumptions are introduced to simplify the process. Indeed, the magnetic gearbox is considered as a regular surface mounted permanent magnet rotor. Accordingly, the torque density τ_v is approximately estimated by reformulating the electromagnetic torque estimation (equation (3.20) and (3.25)):

$$\tau_v = \frac{T_{i_r}}{\pi L_e R_s^2} = \frac{4\sqrt{2}}{\pi} A_L B_{g_{max}} sin(\beta_{m2}\frac{\pi}{2}) \tag{5.11}$$

where T_{i_r} is the rated stator torque, k_f is the winding fill factor, β_{m2} is the ring permanent magnet pitch ratio and the initial torque density is chosen $\tau_v = 40kNm/m^3$.

the second estimation concerns the stack length ratio which is presented by the following equation

$$\epsilon = \frac{L_e}{2R_s} = p_i^{-0.56} \tag{5.12}$$

where p_i is the stator pole pairs number. Considering the two first equations and equation (5.7), the stator diameter or radius can be estimated as below

$$R_s = \sqrt[3]{\left(\frac{T_{i_r}}{2\pi\epsilon\tau_v}\right)} \tag{5.13}$$

where $T_{i_r} = \frac{\gamma T_{m_r}}{u_g}$ and the modulator rated torque is $T_{m0} = 59.46kNm$ which is also the rated input shaft torque. Additional assumptions are cited below:

- The current density $J = 2.5A/mm^2$.
- The current loading $A = 30kA.m$.
- The stator slot height h_s is accordingly calculated basing on eq. (3.25) developed in chapter 3.
- The split factor is chosen equal to $\gamma = 0.8$.
- The tooth pitch ratio β_t, it is fixed at 0.5.
- The stator height yoke h_{ys} is equal to the teeth width $h_{ys} = \beta_t Rs\theta_t$

Rotors sizing

Concerning the magnetic gearbox initial sizing, the following assumptions are considered:

- The two gears magnets heights and the pole pieces height are assumed to be equal $h_{m1} = h_{m2} = h_{mod}$.
- The magnets height are assumed to be the half of the sun gear pole pitch $0.5R_s\theta_{m2}$.
- The pole pitch ratio of both the sun gear and the ring gear are fixed at $\beta_{bm1} = \beta_{m2} = 0.8$. However, the modulator pole pieces pitch ratio are fixed at $\beta_{mod} = 0.5$.
- The rotor yoke heights h_{y1} and h_{y2} are considered equal to the half of their associated rotor pole pitch $h_{y1} = 0.5Rs\theta_{m1}$ and $h_{y2} = 0.5Rs\theta_{m2}$.

5.3.3 Finite element modeling

The finite element modeling is employed during the optimization process using the tool FEMM. two-dimensional Finite element method is used to solve Maxwell equations, which allows the calculation of the magnetic field potential vector in each element. The torque density can be afterwards calculated. Indeed, the stall torque is calculated by using Maxwell stress tensor by only one finite element simulation under rated operating conditions.

5.3.4 Constraints

The optimization process considers a set of possible solutions. This set is described by the following constraints:

- The split factor should be greater or equal to 0.8 ($\gamma \geqslant 0.8$). Indeed, this condition can be reformulated to presents a constraint on the stator rated torque ($\frac{T_{mr}}{u_g} \geqslant T_{i_r} \geqslant \frac{0.8T_{mr}}{u_g}$).
- The current density have to be less than $6A/mm^2$ to avoid the stator overheating.
- To limit the set of possible solutions, every size variable is kept in a limited range.

5.4 Design results

The design optimization is performed by using the tool FEMM. The stall torque of the optimized system is calculated according to the modulator angular position. The following figure 5.5 shows its curve in addition to the calculated steady torque of the sun gear.

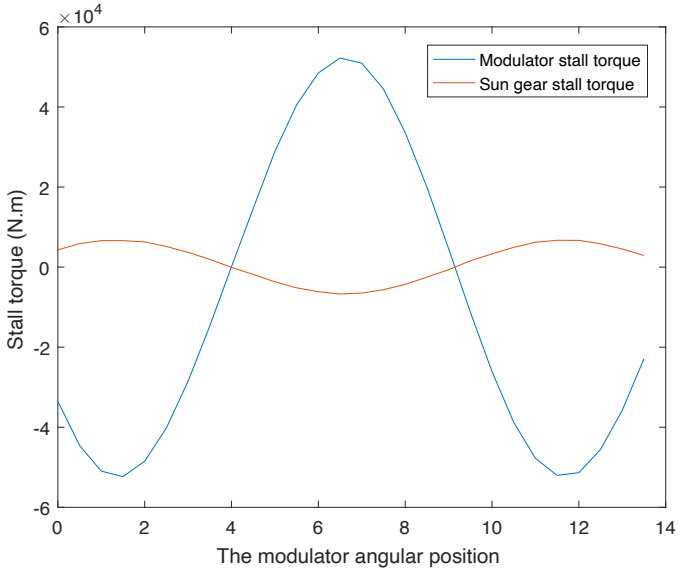

FIGURE 5.5: The PDD calculated stall torque

The obtained optimal design is summarized in the following table 5.1. The Multibrid design parameters and the direct-drive ones are added for comparison.

According to the obtained results, the PDD generator design has an external radius comparable to the Multibrid one, however its estimated cost is almost the same as the direct-drive one. Even if the PDD is not designed in the same way as the direct drive and the Multibrid generator, the comparison shows that the Multibrid system is always the best option. Indeed, the design of the PDD needs more investigations when high power are employed. The saturation phenomena is one of the problems that the magnetically-geared generators suffer from. Concerning the generator efficiency, only iron and copper losses are considered to estimate it. Figure 5.6 shows the flux density of the designed system under full load operating conditions (rated stator current). Such design can be improved by adding a bridge to the modulator, by avoiding corners in the design where the flux density can be saturated. More constraints can be added to improve the design optimization.

TABLE 5.1: Optimal designed parameters of the tidal stream turbine system.

Drivetrain configuration	PDD	D-drive	Multibrid (3:1)
Generator size ($500kW$)			
Generator rated speed [rpm]	80.3	80.3	240.9
Generator rated torque [kN.m]	59.46	59.46	19.82
External radius R_e [m]	0.5596	0.9143	0.6945
Air gap radius R_s [m]	0.5596	0.7420	0.6259
Equivalent core length L_e [m]	0.4586	0.5010	0.6115
Stator tooth pitch ratio β_t	0.71	0.77	0.52
Stator slot height h_s [mm]	64.9	104.6	32
Stator yoke height h_{ys}[mm]	131.8	84.7	37.0
Ring magnet height h_{m2} [mm]	17.0	16 (Rotor)	4 (Rotor)
Modulator pole pieces height h_{mod} [mm]	22.7	-	-
Sun gear magnet height h_{m1} [mm]	28.4		
Modulator pole pieces height h_{mod} [mm]	22.7	-	-
Ring gear rotor yoke height h_{y2} [mm]	102.1	-	-
Sun gear rotor yoke height h_{y1} [mm]	70.3	-	-
Ring gear pole pitch ratio β_{m2}	0.91	-	-
Sun gear pole pitch ratio β_{m1}	0.78	-	-
Modulator pole pieces pitch ratio β_{m1}	0.53	-	-
Torque split factor γ	0.95	-	-
Generator efficiency	0.966	0.954	0.959
system weight [Ton] and cost [k €]			
Iron	5.23	1.06	0.655
Copper	0.908	0.540	0.225
Permanent magnet	0.385	0.340	0.105
Generator weight	6.523	1.94	1.06
Gearbox weight	0	0	0.392
Generator cost	38.8	37.82	10.59
Gearbox cost	0	0	2.35

5.5 Conclusions

Chapter 5 deals with the optimal design of a magnetically-geared generator for tidal turbine applications. Indeed, such topology is proposed in chapter 3 as a promising alternative to conventional generators. In this context, the pseudo-direct drive generator is introduced as a chosen topology, where its operating principles are highlighted. The design optimization was preceded by an initial rough design of the stator and the rotor separately in order to decrease the number of iterations while the searching of the optimum. The optimization cost function is presented by the torque density, where the objective is the compactness of the generator and not the cost. The results show that the size of the PDD generator is relatively similar to the Multibrid one. However, its cost is high and it is close to the direct-drive generator one. Further improvements can be performed on the optimization process as including more constraints and considering the generator cost.

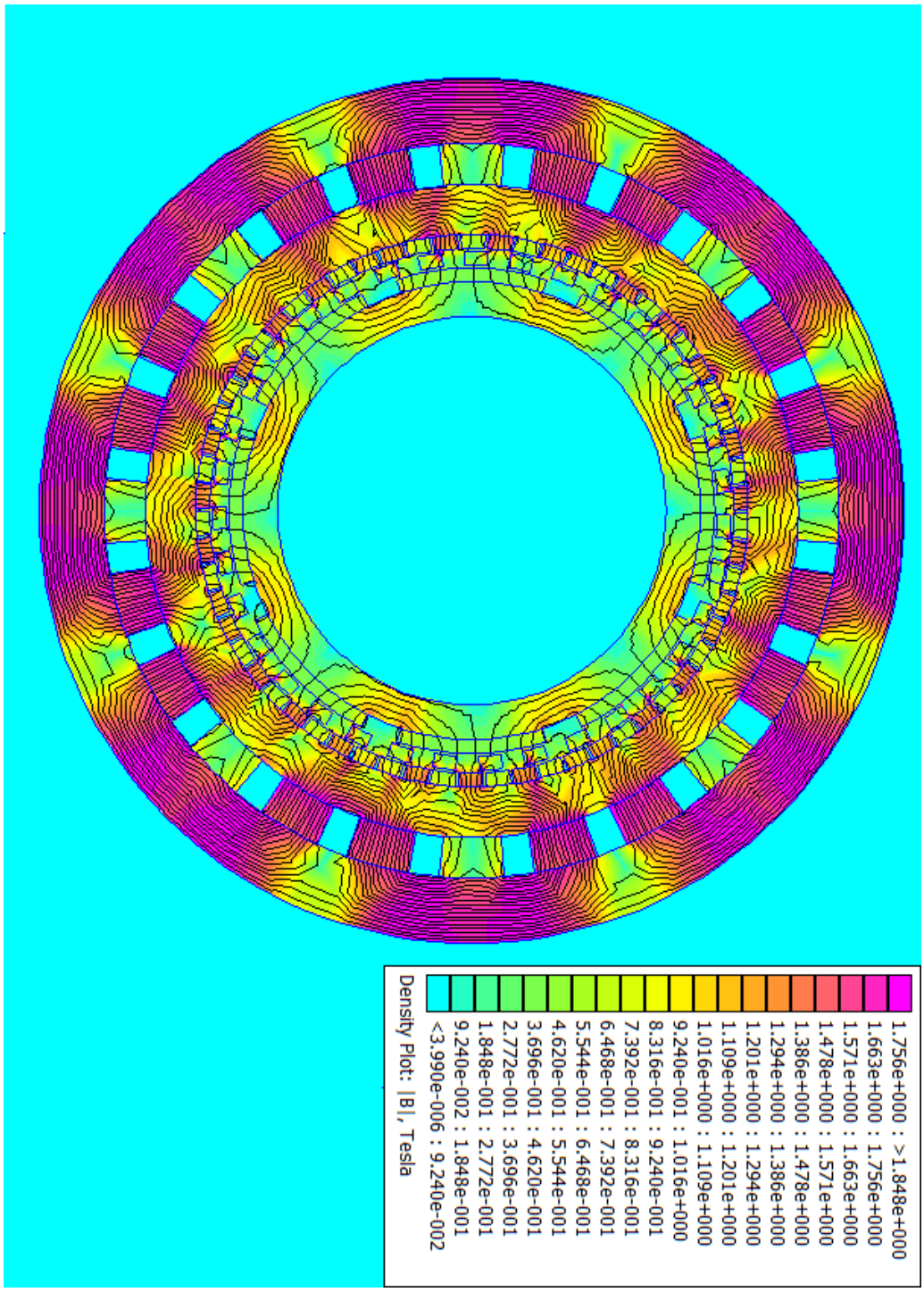

FIGURE 5.6: Flux density and field lines under full load operating conditions

Conclusion and Perspectives

This PhD thesis has addressed the impact of drivetrain configuration choices on the tidal stream turbine reliability, performance, and cost. In this context a review-based comparison is performed between different drivetrain configurations to investigate the appropriate drivetrain configuration for tidal stream turbine applications. For this purpose, the critical drivetrain issues are highlighted basing mostly on wind turbine statistics due to the similarities between wind turbines and tidal stream turbines. The comparison main results show that the gearbox remain being competitive and widely used in wind and marine turbine industry despite its high criticality. Besides that, unconventional geared drivetrains as the Multibrid concept has proven its high availability which makes such configuration highly recommended to be employed for tidal stream applications. However, more investigations on such design should be performed to accelerate its standardization. On the other hand, direct-drive generators presents an interesting alternative to geared systems, especially the permanent magnet ones, due to their high availability. However, such generators operate under high torque and low speed conditions, which makes them large and expensive. Indeed, each drivetrain configuration has its challenges to be more reliable and cost-effective. The direct-drive concept requires more improvements on the generator sizing. Whereas, gearbox driven systems need more improvements on their gearbox to reduce its weight, cost and losses.

In the second chapter, the design models of three types of tidal stream turbines are presented: the two-stage gearbox driven tidal stream turbines, the single-stage gearbox driven one, and the direct-driven one. In addition, the model of the site resource energy is considered, where it is shown that employing a yaw system is not relevant. In this context, a bi-directional axis tidal stream turbine is chosen as option. secondly, it is shown that a power rating of only 30% of the maximum power is sufficient to harness 90% of the total site energy per year. thirdly, the size model of two types of gear stages are proposed (the parallel shaft and the planetary gearbox) for the use in tidal stream turbine applications. Moreover, the generator design is performed with a two-dimensional analytical model, in addition to the rough modeling of the power electronic converter.

The third chapter focuses on the design optimization of the permanent magnet generator basing on the size model proposed in chapter 3. The objective is to investigate the cost-effectiveness of each considered drivetrain configuration. The cost-effectiveness of the gear ratio variation for the same drivetrain configuration is also investigated. Moreover, three power ratings are considered to compare their produced energy in regards to their cost and drivetrain choice. According to the obtained results, the Multibrid concept presents a promising choice when compared to direct-drive and two-stage geared configuration. In addition, a gear ratio of (3:1) is the optimal choice for Multibrid systems, even if (5:1) gear ratio seems also acceptable. Concerning the direct-drive generator, it is shown that the generator presents a great part of its total cost, which requires more investigations to improve its design. On the other hand, the two-stage geared tidal stream turbines have a problem with the gearbox size and cost, which also need more improvements. The estimated cost per produced energy shows similar results for low gear ratios including the direct-drive configuration. However, for high gear ratios the $500kW$ generators are advantageous. Direct-drive configuration have less sensitivity to power rating changes compared to geared ones.

The forth chapter introduces the magnetically-geared generators design for tidal turbines specifications, where the outer-stator magnetically-geared generator topology is chosen to be designed. The Design is based on two-dimensional finite elements analysis and the feasible direction method is adopted as an optimization algorithm. The objective is to maximize the generator toque density while assuring the initial specifications especially the stator rated torque. An initial sizing model is proposed to limit the set of possible solutions and to improve the design process efficiency. The design results show that the PDD generator despite having a low external size, its weight and cost are higher if compared to the Multibrid system. However, it have relatively similar cost comparing to the direct-drive option.

Considering the attained results in this PhD thesis, further future researches can be performed on four axis and they are summarized as bellow:

- The reliability and availability estimation of tidal stream turbine systems is needed as the available reliability data on such turbines is rare. In this context, efficient estimations models can be developed basing on wind turbine reliability data and adapt it for tidal turbines. Such models can be used to estimate more accurately the cost of produced energy as well as the operation and maintenance cost. Otherwise, maintenance cost limitation can be added as a constraint while designing the system.
- The single-stage gearbox is a promising component that can be integrated with permanent magnet generator. Further investigations are required to design the

two components more accurately, especially the gearbox sizing.

- magnetically-geared generators are in the development phase, such technology requires more investigation on the economical and technical feasibility for the use in tidal stream turbine systems. Moreover, the operating point of such generators need to be investigated especially during the power limitation phase.
- The power electronic converters can be considered in the system design process (architecture, control, reliability and availability, cost, impact on the grid if connected to it).

References

[1] Z. Zhou, M. Benbouzid, J.-F. Charpentier, F. Scuiller, and T. Tang, "Developments in large marine current turbine technologies–a review," *Renewable and Sustainable Energy Reviews*, vol. 71, pp. 852–858, 2017.

[2] D. M. Faris Elasha and J. A. Teixeira, "Condition monitoring philosophy for tidal turbines," *International Journal of Performability Engineering*, vol. 10, no. 5, pp. 521–534, 2014.

[3] S. Sheng, "Report on wind turbine subsystem reliability-a survey of various databases/national renewable energy laboratory (nrel)," tech. rep., PR-5000-59111, 2013.

[4] Y. Feng, Y. Qiu, C. J. Crabtree, H. Long, and P. J. Tavner, "Monitoring wind turbine gearboxes," *Wind Energy*, vol. 16, no. 5, pp. 728–740, 2013.

[5] J. Ukonsaari and N. Bennstedt, "Wind turbine gearboxes. maintenance effect on present and future gearboxes for wind turbines," tech. rep., Report 2016:279, ISBN 978-91-7673-279-3, Energieforsk, 2016.

[6] "Seagen tidal turbine," (accessed: 07.05.2020). https://simecatlantis.com/services/turbines/.

[7] "Tidal stream turbine planetary gearbox," (accessed: 07.05.2020). wikov.com/en/mechanical-gearboxes/products/tidal-stream-planetary-gearbox-10314.

[8] Y. Guo, R. Bergua, J. van Dam, J. Jove, and J. Campbell, "Improving wind turbine drivetrain designs to minimize the impacts of non-torque loads," *Wind Energy*, vol. 18, no. 12, pp. 2199–2222, 2015.

[9] "haliade 150-6mw offshore wind turbine," (accessed: 07.05.2020). ge.com/renewableenergy/wind-energy/offshore-wind/offshore-turbine-haliade-150-6mw.

[10] A. Matveev, "Novel pm generators for large wind turbines," in *Wind Power R&D seminar-Deep sea offshore wind power*, 2011.

[11] O. Keysan, "Future electrical generator technologies for offshore wind turbines," *Eng. Technol. Ref*, pp. 1–11, 2015.

[12] S. Djebarri, J. F. Charpentier, F. Scuiller, and M. Benbouzid, "Design and performance analysis of double stator axial flux pm generator for rim driven marine current turbines," *IEEE Journal of Oceanic Engineering*, vol. 41, no. 1, pp. 50–66, 2015.

[13] "Voith hydro tidal stream turbine," (accessed: 07.05.2020). http://www.emec.org.uk/about-us/our-tidal-clients/voith-hydro/.

[14] S. Paboeuf, P. Yen Kai Sun, L.-M. Macadré, and G. Malgorn, "Power performance assessment of the tidal turbine sabella d10 following iec62600-200," in *ASME 2016 35th International Conference on Ocean, Offshore and Arctic Engineering*, American Society of Mechanical Engineers Digital Collection, 2016.

[15] "Areva m5000 wind turbine," (accessed: 07.05.2020). en.wind-turbine-models.com/turbines/23-areva-m5000-116.

[16] Q. Xu, W. Li, Y. Lin, H. Liu, and Y. Gu, "Investigation of the performance of a stand-alone horizontal axis tidal current turbine based on in situ experiment," *Ocean Engineering*, vol. 113, pp. 111–120, 2016.

[17] Y. Lin, L. Tu, H. Liu, and W. Li, "Fault analysis of wind turbines in china," *Renewable and Sustainable Energy Reviews*, vol. 55, pp. 482–490, 2016.

[18] G. Payne, A. Kiprakis, M. Ehsan, W. H. S. Rampen, J. Chick, and A. Wallace, "Efficiency and dynamic performance of digital displacement™ hydraulic transmission in tidal current energy converters," *Proceedings of the Institution of Mechanical Engineers, Part A: Journal of Power and Energy*, vol. 221, no. 2, pp. 207–218, 2007.

[19] H.-w. Liu, W. Li, Y.-g. Lin, and S. Ma, "Tidal current turbine based on hydraulic transmission system," *Journal of Zhejiang University-SCIENCE A*, vol. 12, no. 7, pp. 511–518, 2011.

[20] J. Carroll, A. McDonald, J. Feuchtwang, and D. McMillan, "Drivetrain availability in offshore wind turbines," in *European Wind Energy Association 2014 Annual Conference*, 2014.

[21] "haliade-x 12mw offshore wind turbine," (accessed: 07.05.2020). ge.com/renewableenergy/wind-energy/offshore-wind/haliade-x-offshore-turbine.

[22] "Nova innovation ltd d2t2 tidal stream turbine," (accessed: 07.05.2020). https://www.novainnovation.com/d2t2.

[23] X. Yin, Y. Fang, and P.-D. Pfister, "High-torque-density pseudo-direct-drive permanent-magnet machine with less magnet," *IET Electric Power Applications*, vol. 12, no. 1, pp. 37–44, 2017.

[24] L. Jian, K. Chau, and J. Jiang, "A magnetic-geared outer-rotor permanent-magnet brushless machine for wind power generation," *IEEE Transactions on Industry Applications*, vol. 45, no. 3, pp. 954–962, 2009.

[25] A. Penzkofer and K. Atallah, "Scaling of pseudo direct drives for wind turbine application," *IEEE Transactions on Magnetics*, vol. 52, no. 7, pp. 1–5, 2016.

[26] W. Tian, Z. Mao, and H. Ding, "Design, test and numerical simulation of a low-speed horizontal axis hydrokinetic turbine," *International Journal of Naval Architecture and Ocean Engineering*, vol. 10, no. 6, pp. 782–793, 2018.

[27] S. Djebarri, J. F. Charpentier, F. Scuiller, and M. Benbouzid, "Design methodology of permanent magnet generators for fixed-pitch tidal turbines with overspeed power limitation strategy," *Journal of Ocean Engineering and Science*, 2019.

[28] F. Elasha, D. Mba, M. Togneri, I. Masters, and J. A. Teixeira, "A hybrid prognostic methodology for tidal turbine gearboxes," *Renewable Energy*, vol. 114, pp. 1051–1061, 2017.

[29] Y.-j. Gu, H.-w. Liu, W. Li, Y.-g. Lin, and Y.-j. Li, "Integrated design and implementation of 120-kw horizontal-axis tidal current energy conversion system," *Ocean Engineering*, vol. 158, pp. 338–349, 2018.

[30] A. Mérigaud and J. V. Ringwood, "Condition-based maintenance methods for marine renewable energy," *Renewable and Sustainable Energy Reviews*, vol. 66, pp. 53–78, 2016.

[31] A. Winter, "Differences in fundamental design drivers for wind and tidal turbines," in *OCEANS 2011 IEEE-Spain*, pp. 1–10, IEEE, 2011.

[32] Y. Peng, S. Asgarpoor, W. Qiao, and E. Foruzan, "Fuzzy cost-based fmeca for wind turbines considering condition monitoring systems," in *2016 North American Power Symposium (NAPS)*, pp. 1–6, IEEE, 2016.

[33] Y. Amirat, M. E. H. Benbouzid, E. Al-Ahmar, B. Bensaker, and S. Turri, "A brief status on condition monitoring and fault diagnosis in wind energy conversion systems," *Renewable and sustainable energy reviews*, vol. 13, no. 9, pp. 2629–2636, 2009.

[34] L. Chen and W.-H. Lam, "A review of survivability and remedial actions of tidal current turbines," *Renewable and Sustainable Energy Reviews*, vol. 43, pp. 891–900, 2015.

[35] H. Polinder, F. F. Van der Pijl, G.-J. De Vilder, and P. J. Tavner, "Comparison of direct-drive and geared generator concepts for wind turbines," *IEEE Transactions on energy conversion*, vol. 21, no. 3, pp. 725–733, 2006.

[36] Y.-L. Wang, "A wave energy converter with magnetic gear," *Ocean Engineering*, vol. 101, pp. 101–108, 2015.

[37] S. Sheng, "Wind turbine gearbox reliability database, condition monitoring, and operation and maintenance research update," tech. rep., National Renewable Energy Lab.(NREL), Golden, CO (United States), 2016.

[38] B. Hahn, M. Durstewitz, and K. Rohrig, "Reliability of wind turbines," in *Wind energy*, pp. 329–332, Springer, 2007.

[39] G. Marsh, "Offshore reliability," *Renewable Energy Focus*, vol. 13, no. 3, pp. 62–65, 2012.

[40] G. Marsh, "Turbine producers step into ten league boots," *Renewable energy focus*, vol. 11, no. 4, pp. 46–51, 2010.

[41] R. Bergua, J. Jové, J. Echarte, and R. Boronat, "Pure torque drivetrain design: a proven solution for increasing the wind turbine reliability," in *Brazil Windpower 2014 conference and exhibition*, 2014.

[42] L. Morris, "Direct drive vs. gearbox: progress on both fronts: will the wind turbine technology showdown leave just one technology standing?," *Power Engineering*, vol. 115, no. 3, pp. 38–42, 2011.

[43] G. Bywaters, V. John, J. Lynch, P. Mattila, G. Norton, J. Stowell, M. Salata, O. Labath, A. Chertok, and D. Hablanian, "Northern power systems windpact

drive train alternative design study report," *NREL, Golden, Colorado, Report no. NREL/SR-500-35524*, 2004.

[44] S. Djebarri, J. F. Charpentier, F. Scuiller, and M. Benbouzid, "Comparison of direct-drive pm generators for tidal turbines," in *2014 International Power Electronics and Application Conference and Exposition*, pp. 474–479, IEEE, 2014.

[45] O. Keysan, A. McDonald, M. Mueller, R. Doherty, and M. Hamilton, "C-gen, a lightweight direct drive generator for marine energy converters," 2010.

[46] O. Keysan, A. S. McDonald, and M. Mueller, "A direct drive permanent magnet generator design for a tidal current turbine (seagen)," in *2011 IEEE International Electric Machines & Drives Conference (IEMDC)*, pp. 224–229, IEEE, 2011.

[47] J. Jin, J.-F. Charpentier, and T. Tang, "Preliminary design of a torus type axial flux generator for direct-driven tidal current turbine," in *2014 First international conference on green energy ICGE 2014*, pp. 20–25, IEEE, 2014.

[48] N. Harkati, L. Moreau, M. Zaim, and J.-F. Charpentier, "Low speed doubly salient permanent magnet generator with passive rotor for a tidal current turbine," in *2013 International Conference on Renewable Energy Research and Applications (ICRERA)*, pp. 528–533, IEEE, 2013.

[49] B. Funieru and A. Binder, "Design of a pm direct drive synchronous generator used in a tidal stream turbine," in *2013 International Conference on Clean Electrical Power (ICCEP)*, pp. 197–202, IEEE, 2013.

[50] H. Chen, N. At-Ahmed, M. Machmoum, and M. E.-H. Zam, "Modeling and vector control of marine current energy conversion system based on doubly salient permanent magnet generator," *IEEE Transactions on Sustainable Energy*, vol. 7, no. 1, pp. 409–418, 2015.

[51] e. S. Djebarri, J. F. Charpentier, F. Scuiller, and M. Benbouzid, "A systemic design methodology of pm generators for fixed-pitch marine current turbines," in *2014 First International Conference on Green Energy ICGE 2014*, pp. 32–37, IEEE, 2014.

[52] S. Djebarri, J. F. Charpentier, F. Scuiller, M. Benbouzid, and S. Guemard, "Rough design of a double-stator axial flux permanent magnet generator for a rim-driven marine current turbine," in *2012 IEEE International Symposium on Industrial Electronics*, pp. 1450–1455, IEEE, 2012.

[53] N. J. Baker, S. Cawthorne, E. Hodge, and E. Spooner, "3d modelling of the generator for openhydro's tidal energy system," 2014.

[54] N. D. Laws and B. P. Epps, "Hydrokinetic energy conversion: Technology, research, and outlook," *Renewable and Sustainable Energy Reviews*, vol. 57, pp. 1245–1259, 2016.

[55] H. Li, Z. Chen, and H. Polinder, "Optimization of multibrid permanent-magnet wind generator systems," *IEEE transactions on energy conversion*, vol. 24, no. 1, pp. 82–92, 2009.

[56] A. J. Wieczorek, S. O. Negro, R. Harmsen, G. J. Heimeriks, L. Luo, and M. P. Hekkert, "A review of the european offshore wind innovation system," *Renewable and Sustainable Energy Reviews*, vol. 26, pp. 294–306, 2013.

[57] M. Penalba and J. V. Ringwood, "A review of wave-to-wire models for wave energy converters," *Energies*, vol. 9, no. 7, p. 506, 2016.

[58] M. Umaya, T. Noguchi, M. Uchida, M. Shibata, Y. Kawai, and R. Notomi, "Wind power generation-development status of offshore wind turbines," *Mitsubishi Heavy Industries Technical Review*, vol. 50, no. 3, p. 29, 2013.

[59] H. Liu, Y. Lin, M. Shi, W. Li, H. Gu, Q. Xu, and L. Tu, "A novel hydraulic-mechanical hybrid transmission in tidal current turbines," *Renewable Energy*, vol. 81, pp. 31–42, 2015.

[60] K. Hart, A. McDonald, H. Polinder, E. J. Corr, and J. Carroll, "Improved cost energy comparison of permanent magnet generators for large offshore wind turbines," in *European Wind Energy Association 2014 Annual Conference*, 2014.

[61] S. Benelghali, M. E. H. Benbouzid, and J. F. Charpentier, "Generator systems for marine current turbine applications: A comparative study," *IEEE Journal of Oceanic Engineering*, vol. 37, no. 3, pp. 554–563, 2012.

[62] J. Davila-Vilchis and R. Mishra, "Performance of a hydrokinetic energy system using an axial-flux permanent magnet generator," *Energy*, vol. 65, pp. 631–638, 2014.

[63] A. Lebsir, A. Bentounsi, M. Benbouzid, and H. Mangel, "Electric generators fitted to wind turbine systems: An up-to-date comparative study," 2015.

[64] F. Spinato, P. J. Tavner, G. J. Van Bussel, and E. Koutoulakos, "Reliability of wind turbine subassemblies," *IET Renewable Power Generation*, vol. 3, no. 4, pp. 387–401, 2009.

[65] P. Tavner, G. Van Bussel, and F. Spinato, "Machine and converter reliabilities in wind turbines," 2006.

[66] D. McMillan and G. W. Ault, "Techno-economic comparison of operational aspects for direct drive and gearbox-driven wind turbines," *IEEE Transactions on Energy Conversion*, vol. 25, no. 1, pp. 191–198, 2010.

[67] C. G. Armstrong, "Power transmitting device," 1901. US Pat. 687 292.

[68] H. T. Faus, "Magnetic gearing," 1941. US Pat. 2 243 555.

[69] S. Rand, "Magnetic transmission system," 1970. US Pat. 3 523 204.

[70] M. Hetzel, "Low friction miniature gear drive for transmitting small forces, and method of making same," 1974. US Pat. 3 792 578.

[71] R.-J. Wang and S. Gerber, "Magnetically geared wind generator technologies: Opportunities and challenges," *Applied energy*, vol. 136, pp. 817–826, 2014.

[72] P. Tlali, R. Wang, and S. Gerber, "Magnetic gear technologies: A review," in *2014 International Conference on Electrical Machines (ICEM)*, pp. 544–550, IEEE, 2014.

[73] E. Gouda, S. Mezani, L. Baghli, and A. Rezzoug, "Comparative study between mechanical and magnetic planetary gears," *IEEE Transactions on Magnetics*, vol. 47, no. 2, pp. 439–450, 2010.

[74] M. Filippini and P. Alotto, "Coaxial magnetic gear design and optimization," *IEEE Transactions on Industrial Electronics*, vol. 64, no. 12, pp. 9934–9942, 2017.

[75] J.-X. Shen, H.-Y. Li, H. Hao, M.-J. Jin, and Y.-C. Wang, "Topologies and performance study of a variety of coaxial magnetic gears," *IET Electric Power Applications*, vol. 11, no. 7, pp. 1160–1168, 2017.

[76] B. McGilton, R. Crozier, A. McDonald, and M. Mueller, "Review of magnetic gear technologies and their applications in marine energy," *IET Renewable Power Generation*, vol. 12, no. 2, pp. 174–181, 2017.

[77] K. Atallah and D. Howe, "A novel high-performance magnetic gear," *IEEE Transactions on magnetics*, vol. 37, no. 4, pp. 2844–2846, 2001.

[78] L. Shah, A. Cruden, and B. W. Williams, "A magnetic gear box for application with a contra-rotating tidal turbine," in *2007 7th International Conference on Power Electronics and Drive Systems*, pp. 989–993, IEEE, 2007.

[79] P. O. Rasmussen, T. O. Andersen, F. T. Jorgensen, and O. Nielsen, "Development of a high-performance magnetic gear," *IEEE transactions on industry applications*, vol. 41, no. 3, pp. 764–770, 2005.

[80] S. Gerber and R. Wang, "Evaluation of a prototype magnetic gear," in *2013 IEEE International Conference on Industrial Technology (ICIT)*, pp. 319–324, IEEE, 2013.

[81] N. W. Frank and H. A. Toliyat, "Analysis of the concentric planetary magnetic gear with strengthened stator and interior permanent magnet inner rotor," *IEEE transactions on industry applications*, vol. 47, no. 4, pp. 1652–1660, 2011.

[82] K. Atallah, J. Rens, S. Mezani, and D. Howe, "A novel "pseudo" direct-drive brushless permanent magnet machine," *IEEE Transactions on Magnetics*, vol. 44, no. 11, pp. 4349–4352, 2008.

[83] P. O. Rasmussen, T. V. Frandsen, K. K. Jensen, and K. Jessen, "Experimental evaluation of a motor-integrated permanent-magnet gear," *IEEE Transactions on Industry applications*, vol. 49, no. 2, pp. 850–859, 2013.

[84] R. Wang, L. Brönn, S. Gerber, and P. Tlali, "Design and evaluation of a disc-type magnetically geared pm wind generator," in *4th International Conference on Power Engineering, Energy and Electrical Drives*, pp. 1259–1264, IEEE, 2013.

[85] M. Johnson, M. C. Gardner, H. A. Toliyat, S. Englebretson, W. Ouyang, and C. Tschida, "Design, construction, and analysis of a large-scale inner stator radial flux magnetically geared generator for wave energy conversion," *IEEE Transactions on Industry Applications*, vol. 54, no. 4, pp. 3305–3314, 2018.

[86] M. Johnson, M. C. Gardner, and H. A. Toliyat, "Design and analysis of an axial flux magnetically geared generator," *IEEE transactions on industry applications*, vol. 53, no. 1, pp. 97–105, 2016.

[87] S. Gerber, *Evaluation and design aspects of magnetic gears and magnetically geared electrical machines*. PhD thesis, Stellenbosch: Stellenbosch University, 2015.

[88] K. Touimi, M. Benbouzid, and P. Tavner, "Tidal stream turbines: With or without a gearbox?," *Ocean Engineering*, vol. 170, pp. 74–88, 2018.

[89] "Shom (service hydrographique et ocanographique de la marine), 3d marine tidal currents in fromveur (ouessant island)," 2014.

[90] S. E. B. Elghali, R. Balme, K. Le Saux, M. E. H. Benbouzid, J. F. Charpentier, and F. Hauville, "A simulation model for the evaluation of the electrical power potential harnessed by a marine current turbine," *IEEE Journal of Oceanic Engineering*, vol. 32, no. 4, pp. 786–797, 2007.

[91] T. El Tawil, J. F. Charpentier, and M. Benbouzid, "Tidal energy site characterization for marine turbine optimal installation: Case of the ouessant island in france," *International journal of marine energy*, vol. 18, pp. 57–64, 2017.

[92] A. Bahaj, A. Molland, J. Chaplin, and W. Batten, "Power and thrust measurements of marine current turbines under various hydrodynamic flow conditions in a cavitation tunnel and a towing tank," *Renewable energy*, vol. 32, no. 3, pp. 407–426, 2007.

[93] S. P. Radzevich, *Dudley's handbook of practical gear design and manufacture*. CRC Press, 2012.

[94] F. O. Rourke, F. Boyle, and A. Reynolds, "Marine current energy devices: current status and possible future applications in ireland," *Renewable and Sustainable Energy Reviews*, vol. 14, no. 3, pp. 1026–1036, 2010.

[95] Y. Guo, T. Parsons, R. King, K. Dykes, and P. Veers, "Analytical formulation for sizing and estimating the dimensions and weight of wind turbine hub and drivetrain components," tech. rep., National Renewable Energy Lab.(NREL), Golden, CO (United States), 2015.

[96] J. Cotrell, "Preliminary evaluation of a multiple-generator drive-train configuration for wind turbines: Preprint," 2002.

[97] S. Djebarri, J.-F. CHARPENTIER, F. Scuiller, and M. Benbouzid, "Génératrice à aimants permanents à flux axial à grand diamètre avec entrefer immergé," 2013.

[98] J. Pyrhonen, T. Jokinen, and V. Hrabovcova, *Design of rotating electrical machines*. John Wiley & Sons, 2013.

[99] G. Böhmeke, "Development and operational experience of the wind energy converter wwd-1," in *Proc. 2003 Europ. Wind Energy Conf*, 2003.

[100] I. Boldea, *The Electric Generators Handbook-2 Volume Set*. CRC press, 2005.

[101] T. Miller, M. McGilp, D. Staton, and J. Bremner, "Calculation of inductance in permanent-magnet dc motors," *IEE Proceedings-Electric Power Applications*, vol. 146, no. 2, pp. 129–137, 1999.

[102] J. R. Hendershot and T. J. E. Miller, *Design of brushless permanent-magnet machines*. Motor Design Books Venice, Florida, USA, 2010.

[103] A. Grauers, "Efficiency of three wind energy generator systems," *IEEE Transactions on Energy Conversion*, vol. 11, no. 3, pp. 650–657, 1996.

[104] S. Brisset, *Démarches et outils pour la conception optimale des machines électriques*. PhD thesis, 2007.

[105] Y.-S. Xue, L. Han, H. Li, and L.-D. Xie, "Optimal design and comparison of different pm synchronous generator systems for wind turbines," in *2008*

International Conference on Electrical Machines and Systems, pp. 2448–2453, IEEE, 2008.

[106] S. Gerber and R.-J. Wang, "Design and evaluation of a magnetically geared pm machine," *IEEE Transactions on Magnetics*, vol. 51, no. 8, pp. 1–10, 2015.

[107] P. Tlali, S. Gerber, and R.-J. Wang, "Optimal design of an outer-stator magnetically geared permanent magnet machine," *IEEE Transactions on Magnetics*, vol. 52, no. 2, pp. 1–10, 2015.

[108] D. Evans and Z. Zhu, "Optimal torque matching of a magnetic gear within a permanent magnet machine," in *2011 IEEE International Electric Machines & Drives Conference (IEMDC)*, pp. 995–1000, IEEE, 2011.

[109] Z. Zhu and D. Howe, "Influence of design parameters on cogging torque in permanent magnet machines," *IEEE Transactions on energy conversion*, vol. 15, no. 4, pp. 407–412, 2000.

[110] N. W. Frank and H. A. Toliyat, "Gearing ratios of a magnetic gear for marine applications," in *2009 IEEE Electric Ship Technologies Symposium*, pp. 477–481, IEEE, 2009.

[111] N. W. Frank and H. A. Toliyat, "Gearing ratios of a magnetic gear for wind turbines," in *2009 IEEE International Electric Machines and Drives Conference*, pp. 1224–1230, IEEE, 2009.

DOCTORAT BRETAGNE SCIENCES LOIRE POUR L'INGENIEUR

Université de Bretagne Occidentale

Titre : Conception optimale d'une hydrolienne associée à un multiplicateur de vitesse

Mots clés : Hydrolienne, concept d'entraînement direct, concept Multibrid, génératrice à aimants permanents, conception optimale

Résumé : L'énergie marémotrice fait l'objet d'une attention croissante en tant que future source potentielle d'énergie renouvelable. Les hydroliennes sont cependant encore en phase de développement et leur technologie n'est pas aussi mature que celle des éoliennes. Outre le fait que cette technologie est encore émergente, les hydroliennes doivent faire face à l'environnement sous-marin hostile dans lequel elles sont immergées. Ces contraintes augmentent la criticité des sous-systèmes des hydroliennes et les rendent moins fiables. Par conséquent, l'amélioration de la fiabilité constitue l'un des défis à relever pour rendre l'énergie marémotrice compétitive en termes de coût par rapport à d'autres types d'énergie, notamment les énergies éolienne et solaire. En effet, la fiabilité des hydroliennes et le coût de l'énergie produite sont principalement affectés par les choix de configuration de la chaîne de conversion d'énergie (entraînement mécanique) et de la génératrice.

Dans cette thèse, le type d'entrainement mécanique le plus adapté aux spécifications des hydroliennes est étudié. Trois configurations principales de génératrices et de transmission sont considérées ; à savoir l'hydrolienne à entraînement direct (sans multiplicateur), l'hydrolienne à multiplicateur mécanique et enfin l'hydrolienne à multiplicateur magnétique. Le processus de conception adopté prend en compte la modélisation électromagnétique de la génératrice, le modèle du convertisseur, le modèle de la turbine et les données de vitesse des courants de marées (près de l'île d'Ouessant).
Les résultats obtenus à l'issue de ces travaux pourraient être utiles aux concepteurs d'hydroliennes et pourraient leur donner un aperçu sur la faisabilité de chaque type de configuration d'hydroliennes.

Title: Optimal design of a gearbox driven tidal stream turbine

Keywords: Tidal stream turbine, direct-drive concept, Multibrid concept, permanent magnet generator, design optimization

Abstract: Tidal stream energy is acquiring more and more attention as a future potential renewable energy source. However, tidal stream turbines are still in development stages and their technology is not as mature as wind turbine technology. In addition to the infancy of the technology, tidal stream turbines have to withstand the harsh submarine environment where they are immersed. These constraints increase the criticality of tidal stream turbine subsystems and make them less reliable. Therefore, improving the reliability presents one of the challenges to make such energy competitive in terms of cost compared to other types, notably wind and solar energies. Indeed, the tidal stream turbine reliability and the produced energy cost are mainly affected by the drivetrain and generator configuration choices.

In this Ph.D. thesis, suitable drivetrain and generator option choice is investigated for tidal stream turbine specifications. Three main generator and drivetrain configurations are considered which are, the direct-drive tidal stream turbine (gearless), the mechanically geared tidal stream turbine, and the magnetically geared one. The design process considers the electromagnetic modeling of the generator, the converter model, the turbine model, and the tidal current velocity data (near Ouessant island).
The investigation-achieved results could be useful for tidal stream turbine designers and could give them a sight on the feasibility of each tidal stream turbine type.